



Cross-correlating galaxy catalogs and GW

A tomographic approach

5ème Assemblée Générale GDR Ondes Gravitationnelles – 11/10/2021

Francesca Calore (CNRS/LAPTh)

In collaboration with *A. Cuoco* (U. Torino), *T. Regimbau* (CNRS/LAPP), *S. Sachdev* (Penn State U.), and *P. D. Serpico* (CNRS/LAPTh)
Based on *Phys. Rev. Research* 2 (2020), [arXiv:2002.02466](https://arxiv.org/abs/2002.02466)

Why cross-correlation of galaxies with GW?

- **X-correlation of galaxy surveys with GW catalogs or the stochastic background** is an example of synergy between cosmology and MM astronomy
- It has been used so far mostly to (i) infer **cosmological parameters**, (ii) constrain **BBH progenitors**, and (iii) disentangle a **primordial BH origin** of BBH events
- This latter goal relies on the possibility to precisely measure the **linear bias**, b , and eventually its redshift evolution

Why cross-correlation of galaxies with GW?

- **X-correlation** of **galaxy surveys** with **GW catalogs** or the **stochastic background** is an example of synergy between cosmology and MM astronomy
- It has been used so far mostly to (i) infer **cosmological parameters**, (ii) constrain **BBH progenitors**, and (iii) disentangle a **primordial BH origin** of BBH events
- This latter goal relies on the possibility to precisely measure the **linear bias**, b , and eventually its redshift evolution

Considering the ***number density fluctuations*** in a population of discrete objects in Fourier space

$$\delta_i(k, z) = b_i(z) \delta_m(k, z)$$

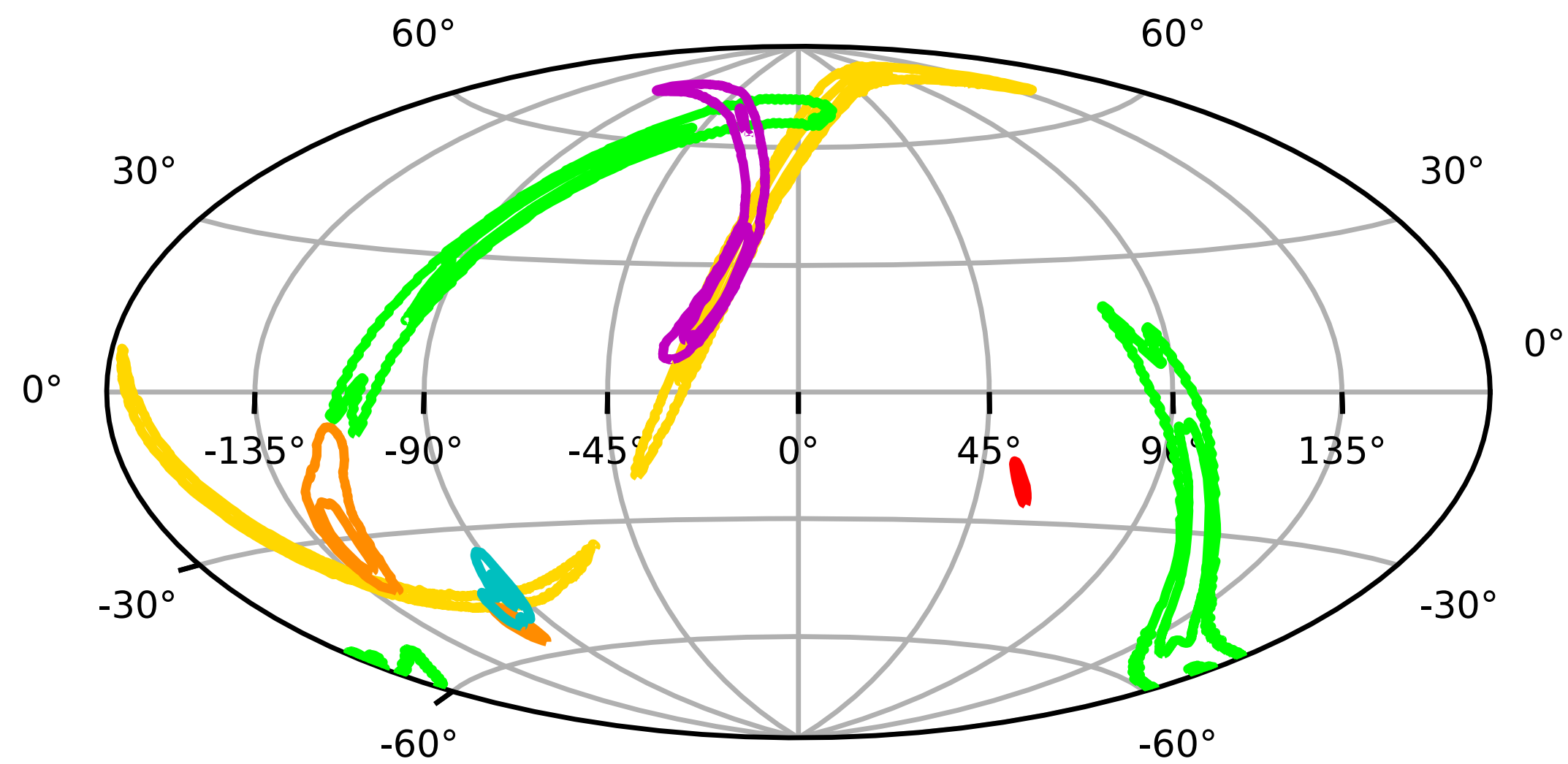
Bias, b , indicates the extent to which the field i traces LSS

- $b > 1$: *Stellar origin*, BBH harboured in luminous and massive galaxies
- $b < 1$: *Primordial origin*, BBH tracing dark matter (known biased tracer of LSS)

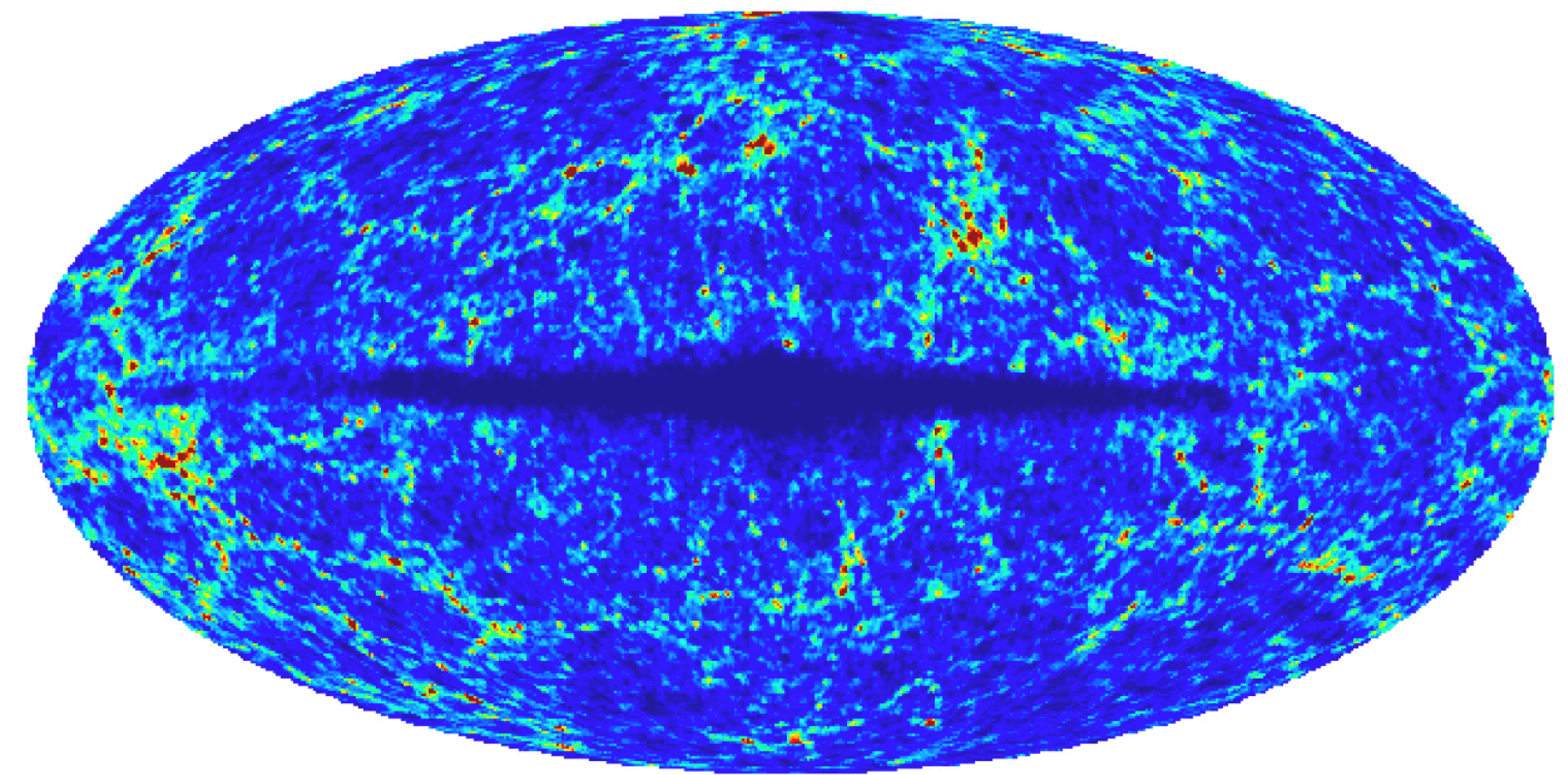
The question

When will we be able to measure the x-correlation between binary events and LSS?

GW event catalogs

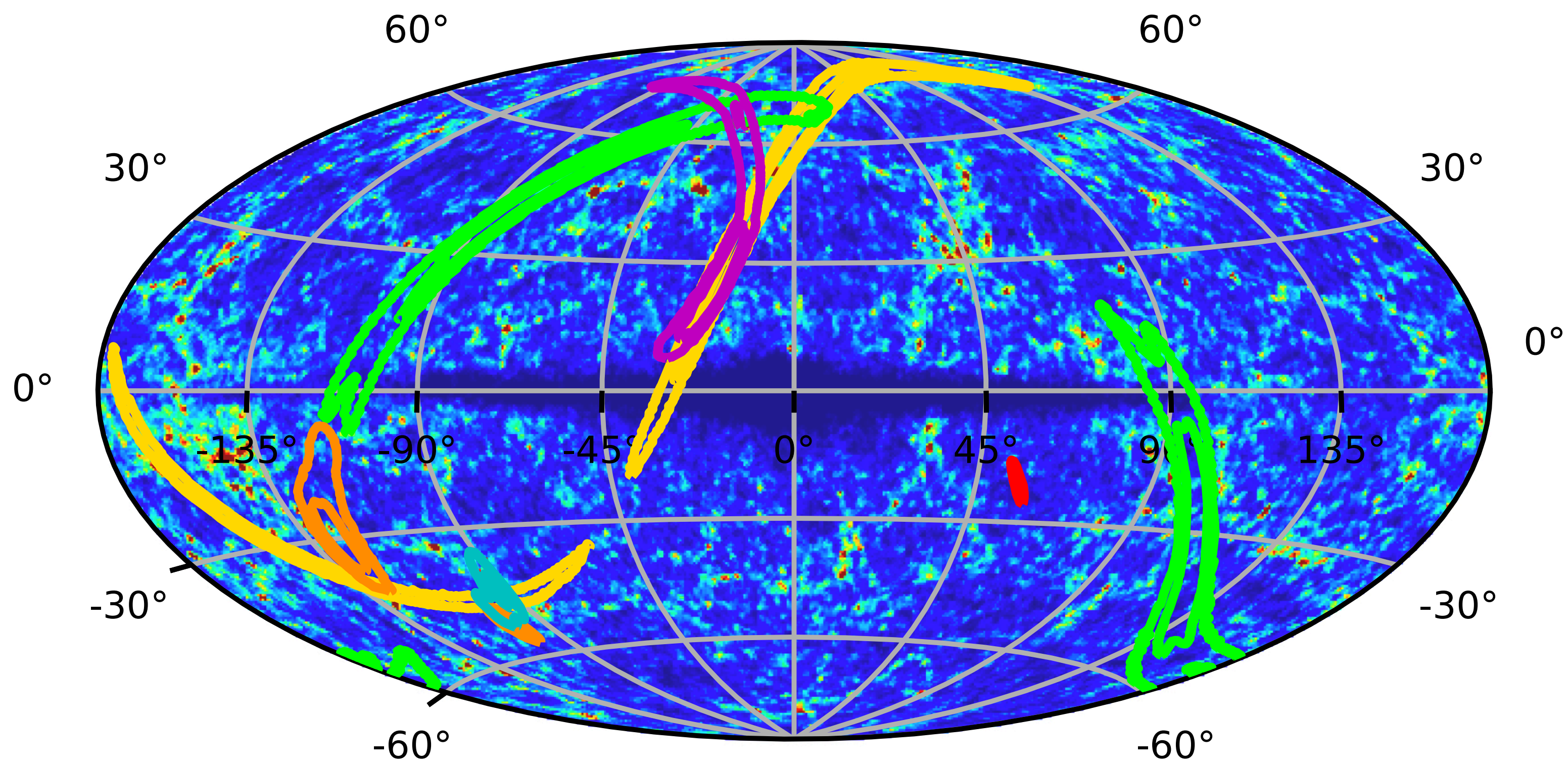


Galaxy catalogs



The answer

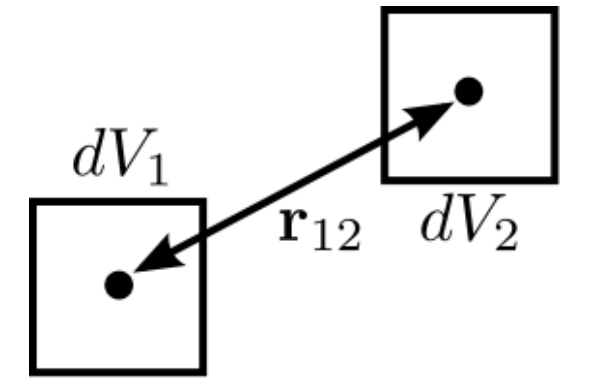
With 10yr of HLVIK at design sensitivity *we can detect* x-correlation of binary populations with LSS



Game changer: galaxy catalog optimisation and tomography

Methodology and formalism

Cross angular power spectrum (CAPS)



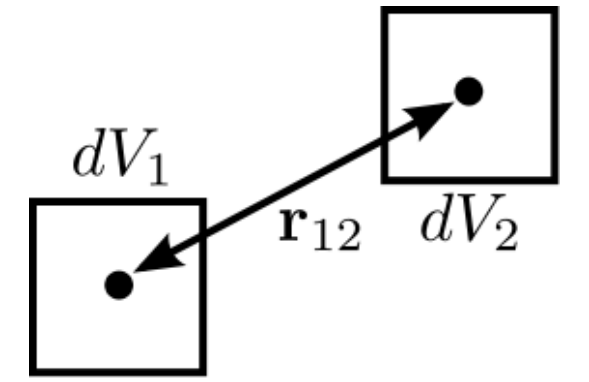
Between number density fluctuations in a population of discrete objects of two catalogs a and b

$$C_{\ell}^{ab} = \frac{2}{\pi} \int k^2 G_{a,\ell}(k) G_{b,\ell}(k) dk$$

$$C_{\ell}^{ab} = \int \frac{d\chi}{\chi^2} P \left(k = \frac{\ell}{\chi}, z(\chi) \right) \prod_{i=a,b} W_i(\chi) b_i(z(\chi))$$

Methodology and formalism

Cross angular power spectrum (CAPS)



Between number density fluctuations in a population of discrete objects of two catalogs a and b

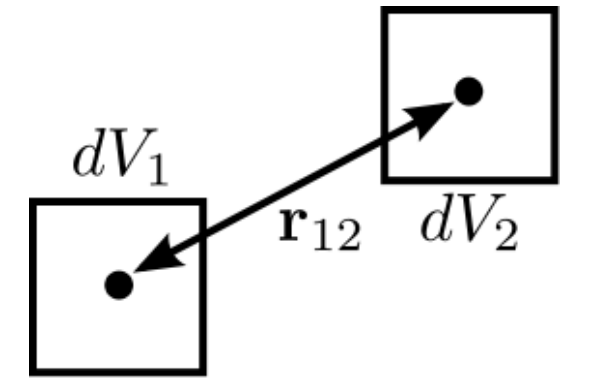
$$C_{\ell}^{ab} = \frac{2}{\pi} \int k^2 G_{a,\ell}(k) G_{b,\ell}(k) dk$$

$$C_{\ell}^{ab} = \int \frac{d\chi}{\chi^2} P \left(k = \frac{\ell}{\chi}, z(\chi) \right) \prod_{i=a,b} W_i(\chi) b_i(z(\chi))$$

Non-linear matter power spectrum of LSS

Methodology and formalism

Cross angular power spectrum (CAPS)



Between number density fluctuations in a population of discrete objects of two catalogs a and b

$$C_{\ell}^{ab} = \frac{2}{\pi} \int k^2 G_{a,\ell}(k) G_{b,\ell}(k) dk$$

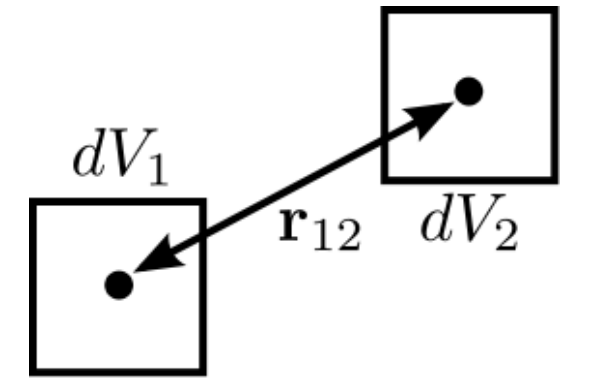
$$C_{\ell}^{ab} = \int \frac{d\chi}{\chi^2} P\left(k = \frac{\ell}{\chi}, z(\chi)\right) \prod_{i=a,b} W_i(\chi) b_i(z(\chi))$$

Non-linear matter power spectrum of LSS

Window function of the field i (catalog redshift distribution)

Methodology and formalism

Cross angular power spectrum (CAPS)



Between number density fluctuations in a population of discrete objects of two catalogs a and b

$$C_\ell^{ab} = \frac{2}{\pi} \int k^2 G_{a,\ell}(k) G_{b,\ell}(k) dk$$

$$C_\ell^{ab} = \int \frac{d\chi}{\chi^2} P\left(k = \frac{\ell}{\chi}, z(\chi)\right) \prod_{i=a,b} W_i(\chi) b_i(z(\chi))$$

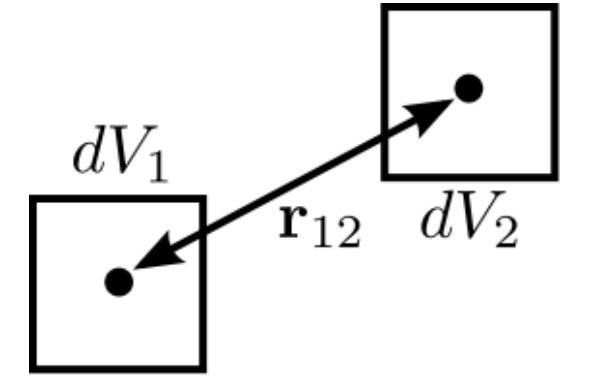
Non-linear matter power spectrum of LSS

Window function of the field i (catalog redshift distribution)

Bias with respect to matter distribution (reference $b = 1$)

Methodology and formalism

Cross angular power spectrum (CAPS)



Between number density fluctuations in a population of discrete objects of two catalogs a and b

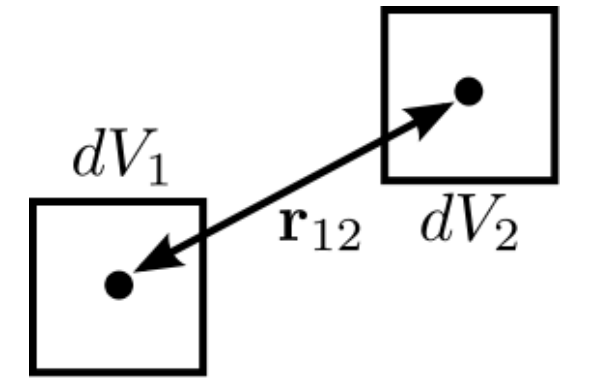
$$C_{\ell}^{ab} = \frac{2}{\pi} \int k^2 G_{a,\ell}(k) G_{b,\ell}(k) dk$$

$$C_{\ell}^{ab} = \int \frac{d\chi}{\chi^2} P \left(k = \frac{\ell}{\chi}, z(\chi) \right) \prod_{i=a,b} W_i(\chi) b_i(z(\chi))$$

$$\left(\frac{\delta C_{\ell}^{ab}}{C_{\ell}^{ab}} \right)^2 = \frac{1}{(2\ell + 1) \Delta \ell f_{\text{fov}}} \left[1 + \frac{C_{\ell}^{aa} C_{\ell}^{bb}}{(C_{\ell}^{ab})^2} \times \left(1 + \frac{C_N^{aa}}{W_{\ell,a}^2 C_{\ell}^{aa}} \right) \left(1 + \frac{C_N^{bb}}{W_{\ell,b}^2 C_{\ell}^{bb}} \right) \right]$$

Methodology and formalism

Cross angular power spectrum (CAPS)



Between number density fluctuations in a population of discrete objects of two catalogs a and b

$$C_{\ell}^{ab} = \frac{2}{\pi} \int k^2 G_{a,\ell}(k) G_{b,\ell}(k) dk$$

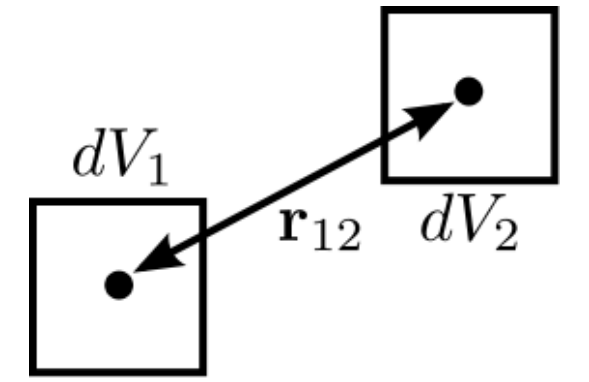
$$C_{\ell}^{ab} = \int \frac{d\chi}{\chi^2} P \left(k = \frac{\ell}{\chi}, z(\chi) \right) \prod_{i=a,b} W_i(\chi) b_i(z(\chi))$$

$$\left(\frac{\delta C_{\ell}^{ab}}{C_{\ell}^{ab}} \right)^2 = \frac{1}{(2\ell + 1) \Delta \ell f_{\text{fov}}} \left[1 + \frac{C_{\ell}^{aa} C_{\ell}^{bb}}{(C_{\ell}^{ab})^2} \times \left(1 + \frac{C_N^{aa}}{W_{\ell,a}^2 C_{\ell}^{aa}} \right) \left(1 + \frac{C_N^{bb}}{W_{\ell,b}^2 C_{\ell}^{bb}} \right) \right]$$

Catalog sky coverage $f_{\text{fov}} \equiv \frac{\Omega_{\text{fov}}}{4\pi}$

Methodology and formalism

Cross angular power spectrum (CAPS)



Between number density fluctuations in a population of discrete objects of two catalogs a and b

$$C_{\ell}^{ab} = \frac{2}{\pi} \int k^2 G_{a,\ell}(k) G_{b,\ell}(k) dk$$

$$C_{\ell}^{ab} = \int \frac{d\chi}{\chi^2} P \left(k = \frac{\ell}{\chi}, z(\chi) \right) \prod_{i=a,b} W_i(\chi) b_i(z(\chi))$$

$$\left(\frac{\delta C_{\ell}^{ab}}{C_{\ell}^{ab}} \right)^2 = \frac{1}{(2\ell + 1) \Delta\ell f_{\text{fov}}} \left[1 + \frac{C_{\ell}^{aa} C_{\ell}^{bb}}{(C_{\ell}^{ab})^2} \times \left(1 + \frac{C_N^{aa}}{W_{\ell,a}^2 C_{\ell}^{aa}} \right) \left(1 + \frac{C_N^{bb}}{W_{\ell,b}^2 C_{\ell}^{bb}} \right) \right]$$

Catalog sky coverage $f_{\text{fov}} \equiv \frac{\Omega_{\text{fov}}}{4\pi}$

Poisson noise $C_N^{ii} \equiv \frac{\Omega_{\text{fov}}}{N_i}$

Mock GW catalogs

Populations of compact binary mergers

1. Monte Carlo code developed for the Einstein Mock data challenges

T. Regimbau et al., Phys. Rev. D86 (2012)

B. P. Abbott et al. Phys. Rev. X 9 (2019)

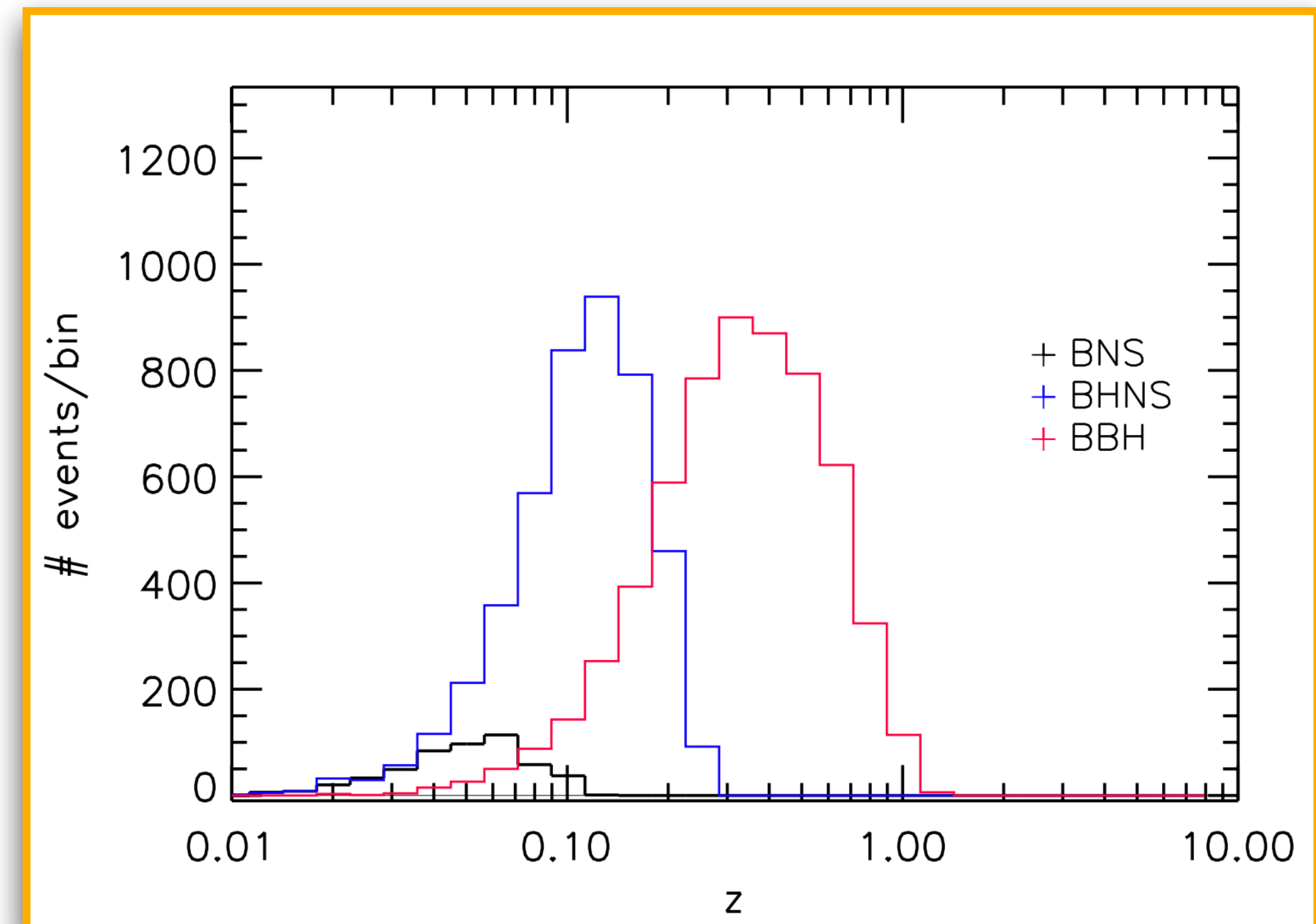
2. Match-filtered signal-to-noise ratio, SNR , for three detector configurations

Binary populations

Detectors

Case	BNS	BBH	BHNS
HLV	5×10^2	4×10^3	$< 2 \times 10^3$
HLVIK	2.5×10^3	2×10^4	$< 2 \times 10^4$
ET2CE	7×10^6	7×10^5	$< 5 \times 10^6$

*# events with $SNR > 8$
for 10yr-data at 80% duty cycle*



Mock GW catalogs

Populations of compact binary mergers

1. Monte Carlo code developed for the Einstein Mock data challenges

T. Regimbau et al., Phys. Rev. D86 (2012)

B. P. Abbott et al. Phys. Rev. X 9 (2019)

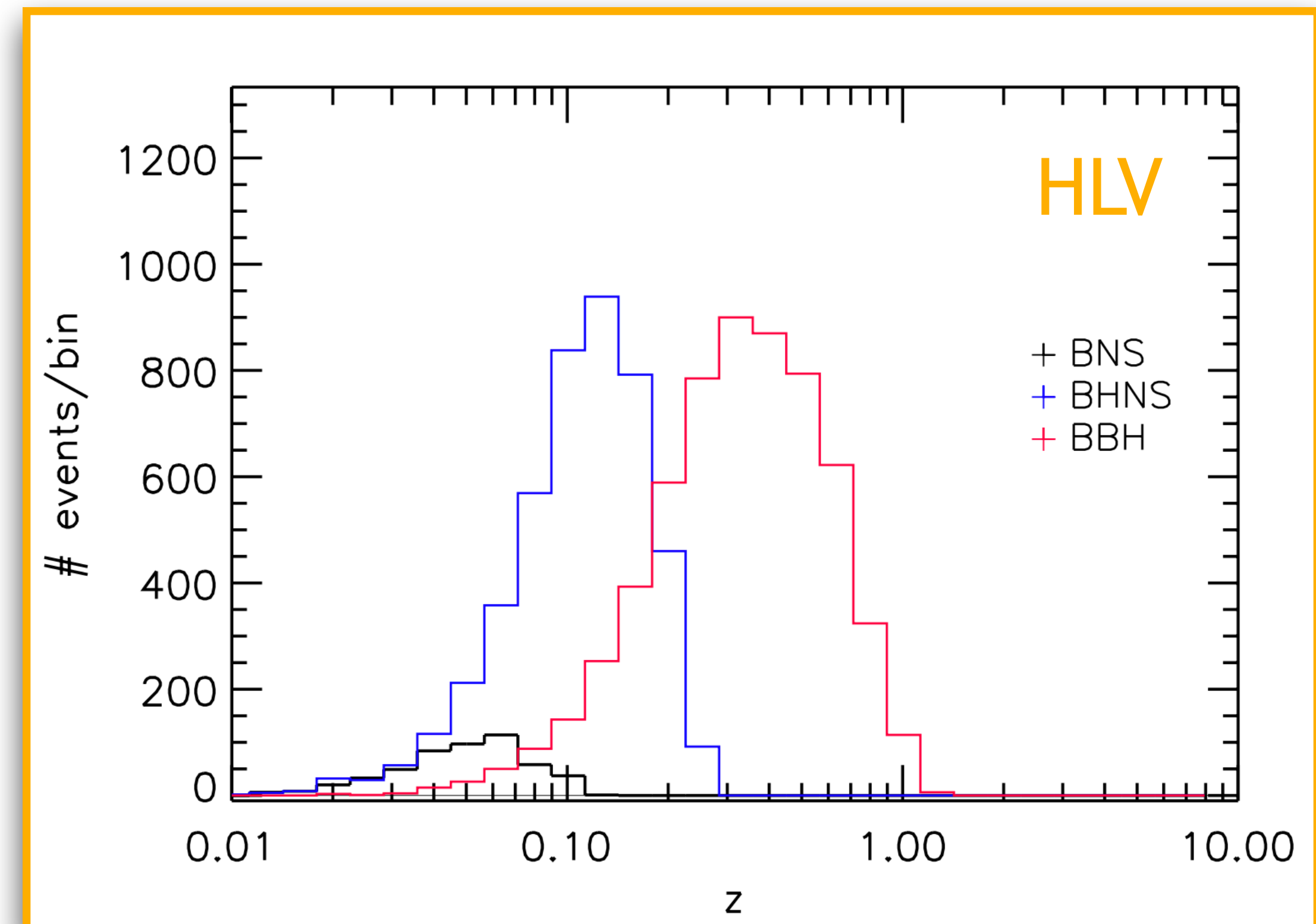
2. Match-filtered signal-to-noise ratio, SNR , for three detector configurations

Binary populations

Detectors

Case	BNS	BBH	BHNS
HLV	5×10^2	4×10^3	$< 2 \times 10^3$
HLVIK	2.5×10^3	2×10^4	$< 2 \times 10^4$
ET2CE	7×10^6	7×10^5	$< 5 \times 10^6$

*# events with $SNR > 8$
for 10yr-data at 80% duty cycle*



Mock GW catalogs

Populations of compact binary mergers

1. Monte Carlo code developed for the Einstein Mock data challenges

T. Regimbau et al., Phys. Rev. D86 (2012)

B. P. Abbott et al. Phys. Rev. X 9 (2019)

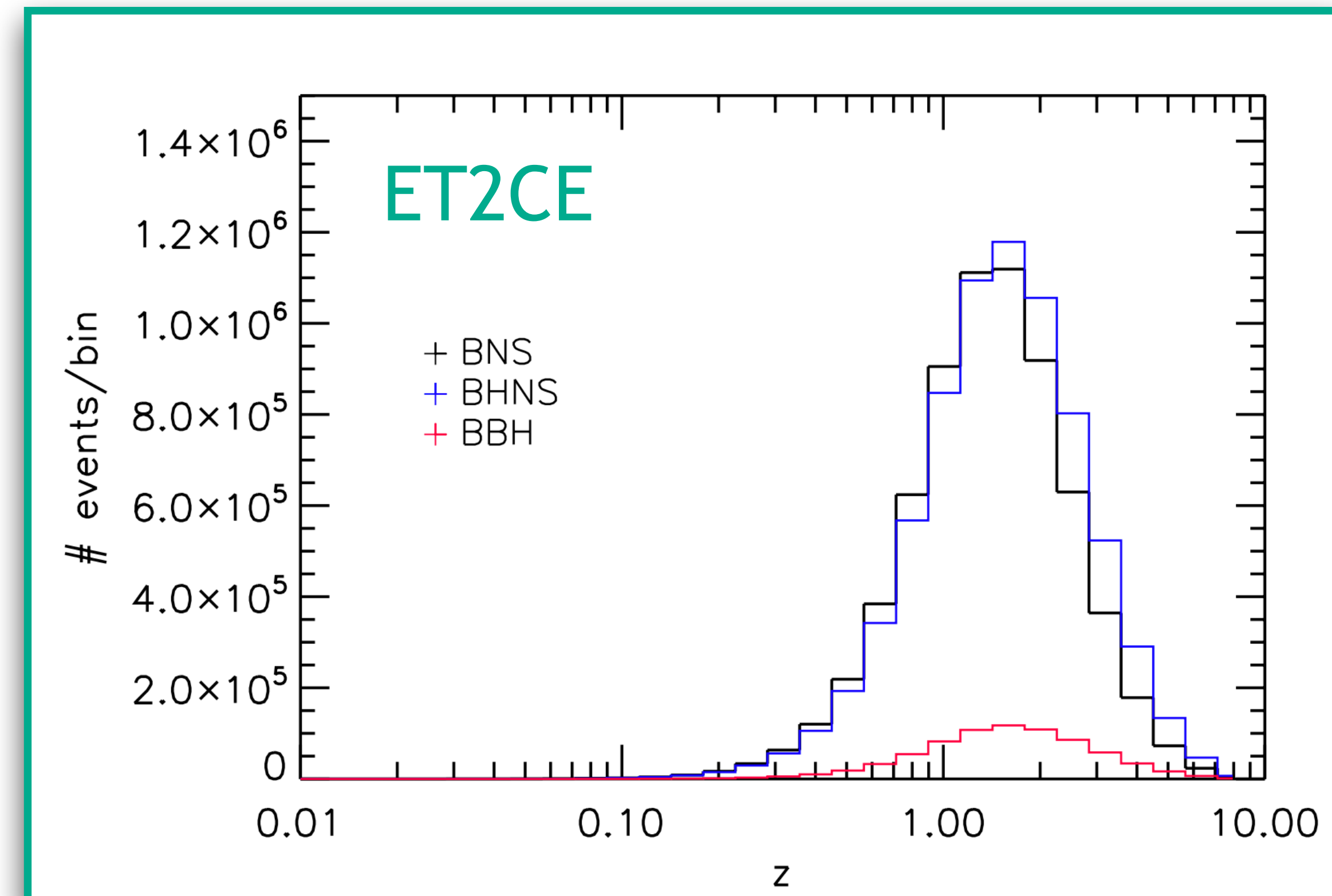
2. Match-filtered signal-to-noise ratio, SNR , for three detector configurations

Binary populations

Detectors

Case	BNS	BBH	BHNS
HLV	5×10^2	4×10^3	$< 2 \times 10^3$
HLVIK	2.5×10^3	2×10^4	$< 2 \times 10^4$
ET2CE	7×10^6	7×10^5	$< 5 \times 10^6$

events with $SNR > 8$
for 10yr-data at 80% duty cycle



Mock GW catalogs

Populations of compact binary mergers

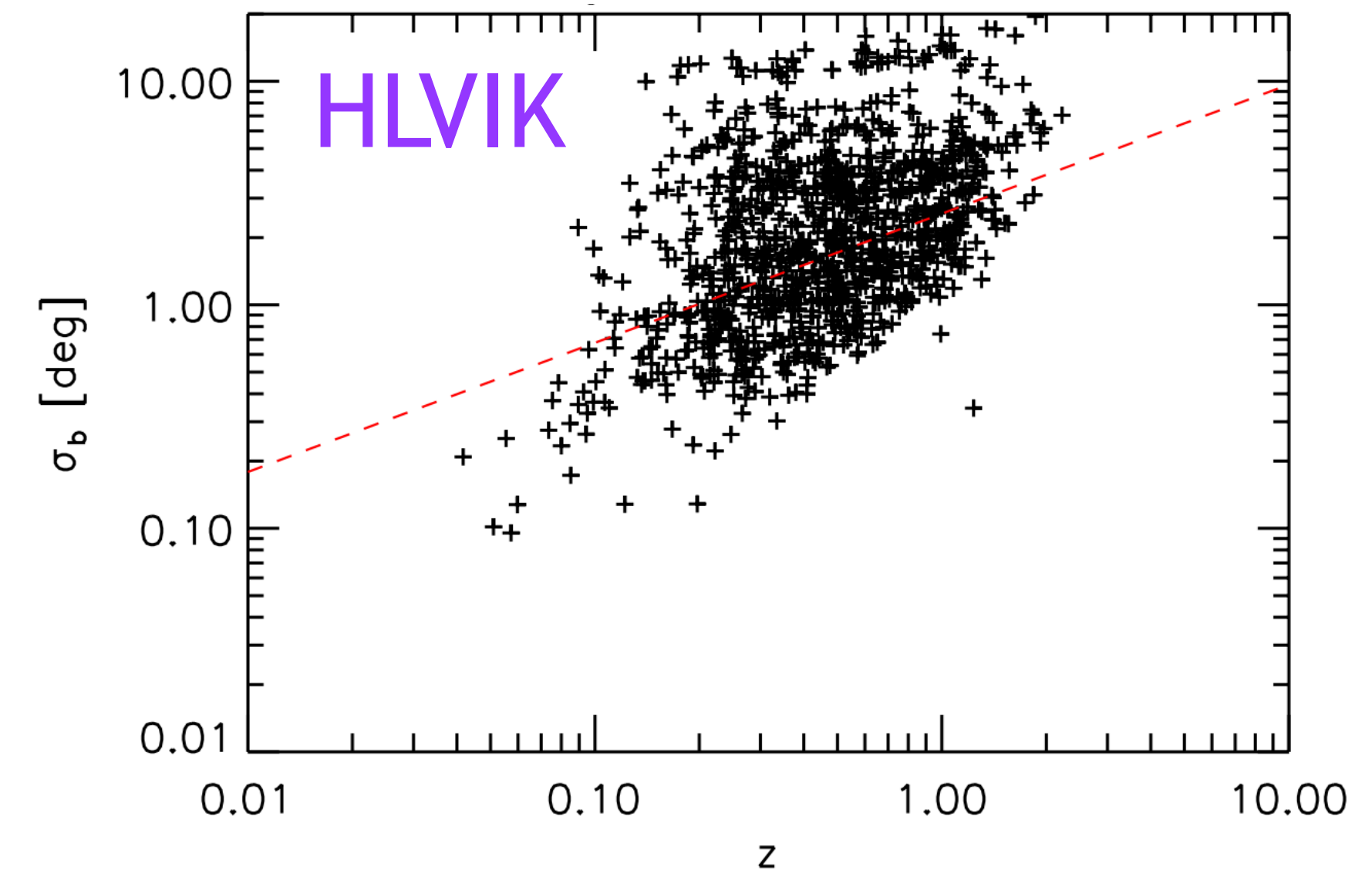
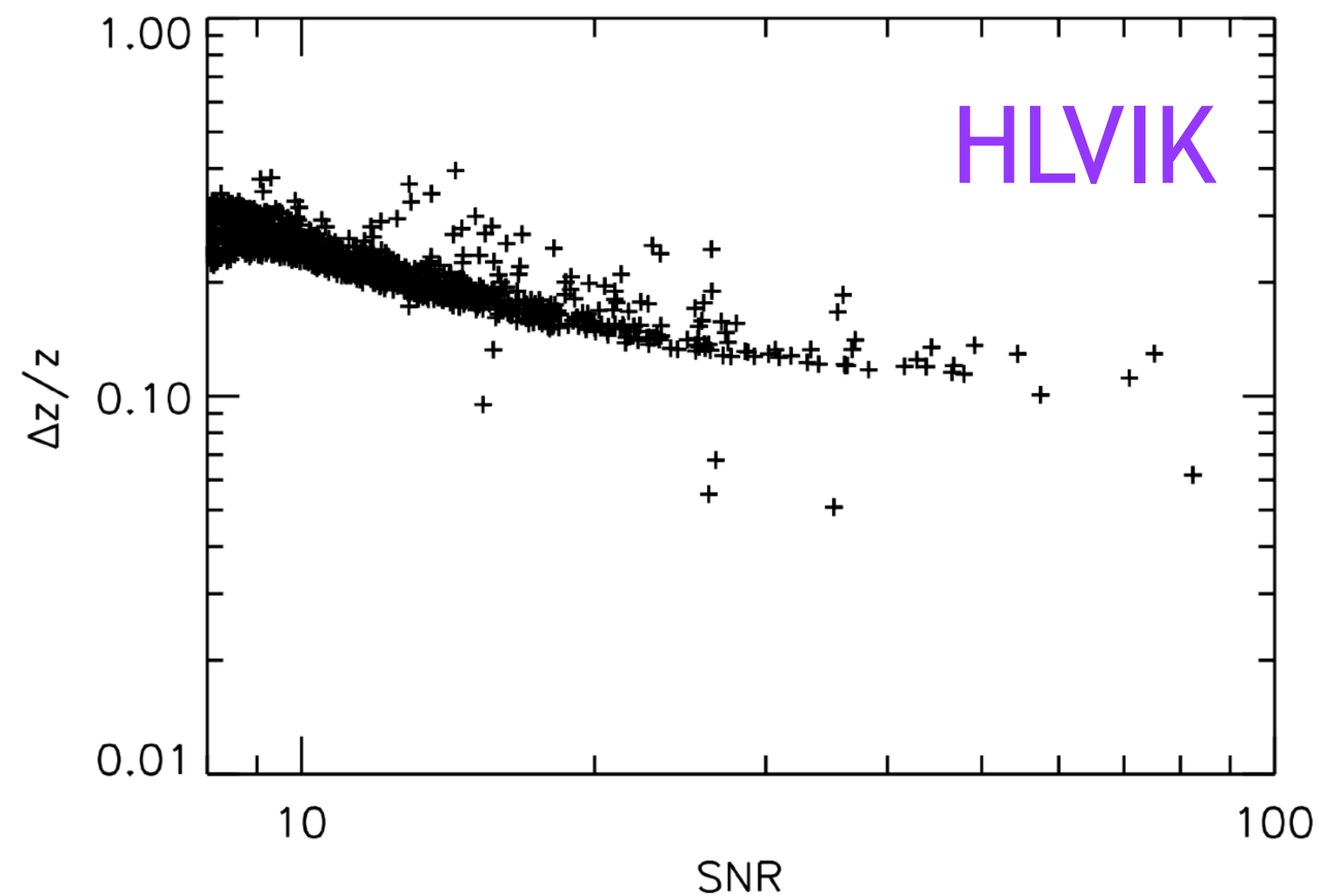
1. Monte Carlo code developed for the Einstein Mock data challenges

T. Regimbau et al., Phys. Rev. D86 (2012)

B. P. Abbott et al. Phys. Rev. X 9 (2019)

2. Match-filtered signal-to-noise ratio, SNR , for three detector configurations

3. Sky localisation and luminosity distance posteriors from BAYESTAR to
(i) redshift error, and (ii) circular Gaussian beam width equivalent

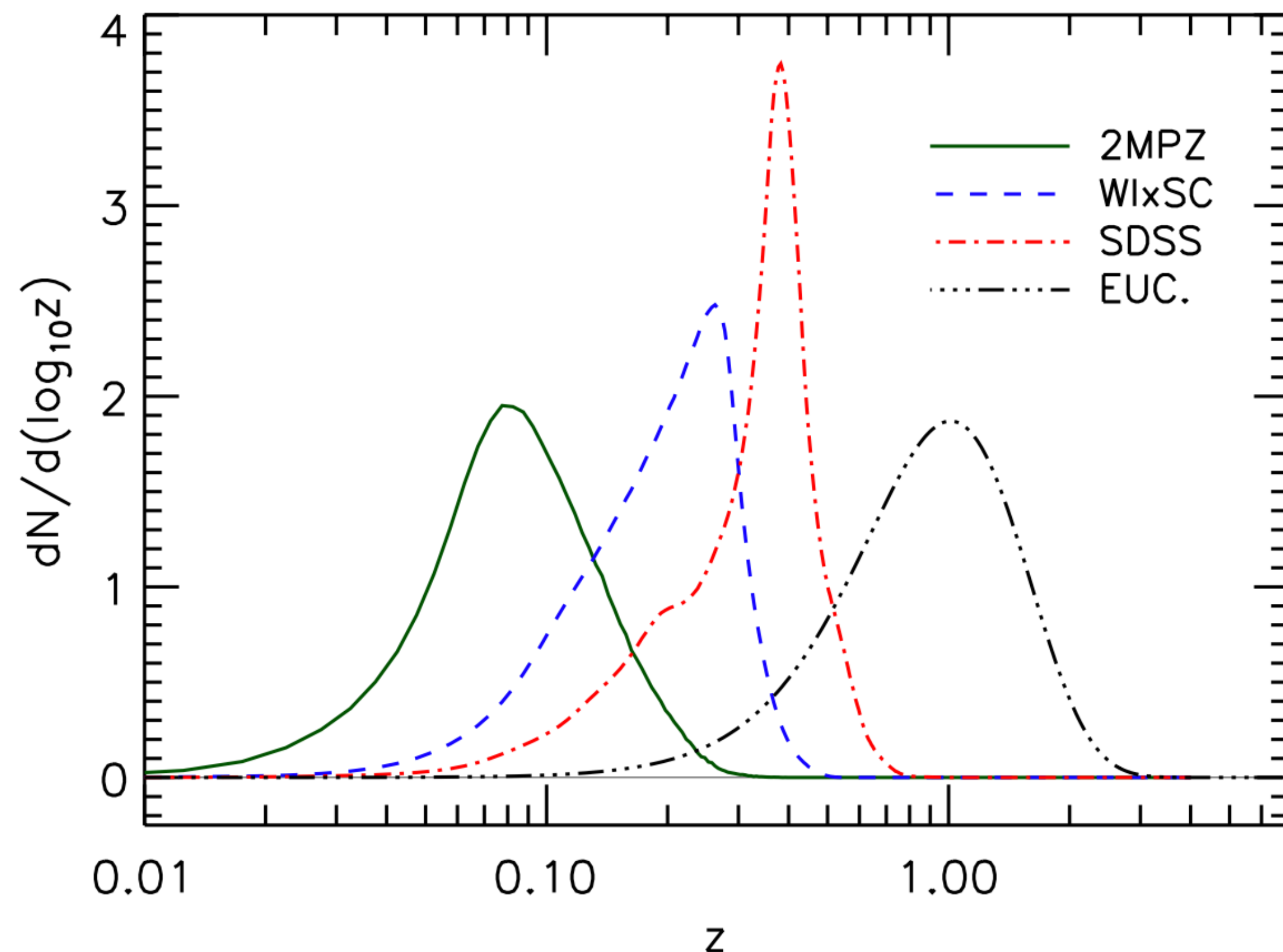


The galaxy catalogs

To reduce the *error on the x-correlation*, we want:

1. Large sky coverage
2. Large number of galaxies

Source redshift distribution



A. Cuoco et al., Astrophys. J. Suppl. 232, 1 (2017); L. Amendola et al., Living Rev. Rel. 21 (2018)

Current catalogs:

a. **2MASS photometric redshift catalog**

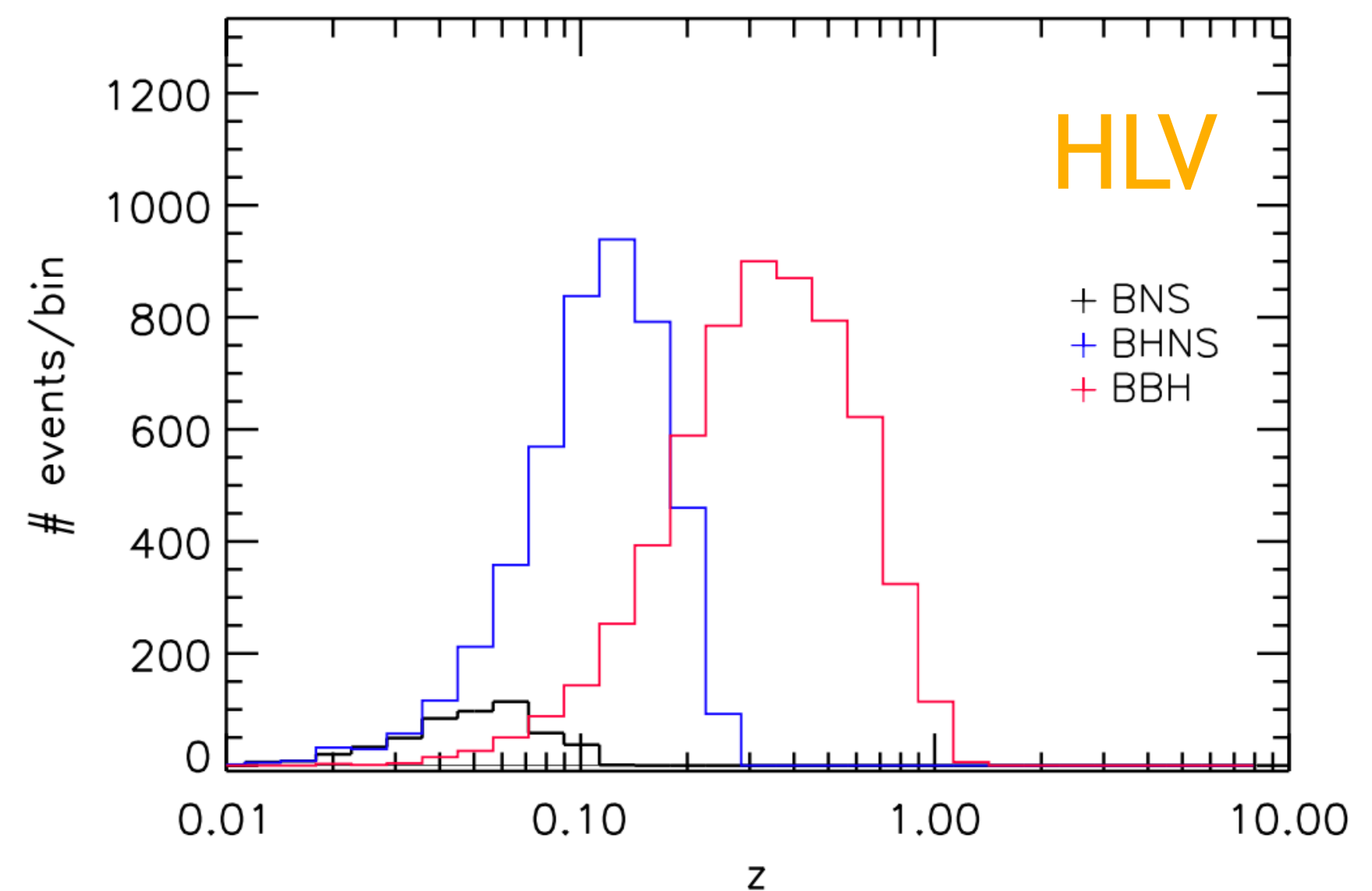
70% sky coverage, $\sim 8 \times 10^5$ galaxies

b. **WISExSuperCosmos**

70% sky coverage, $\sim 2 \times 10^7$ galaxies

c. **SDSS Data Release 12 photometric catalog**

20% sky coverage, $\sim 10^7$ galaxies

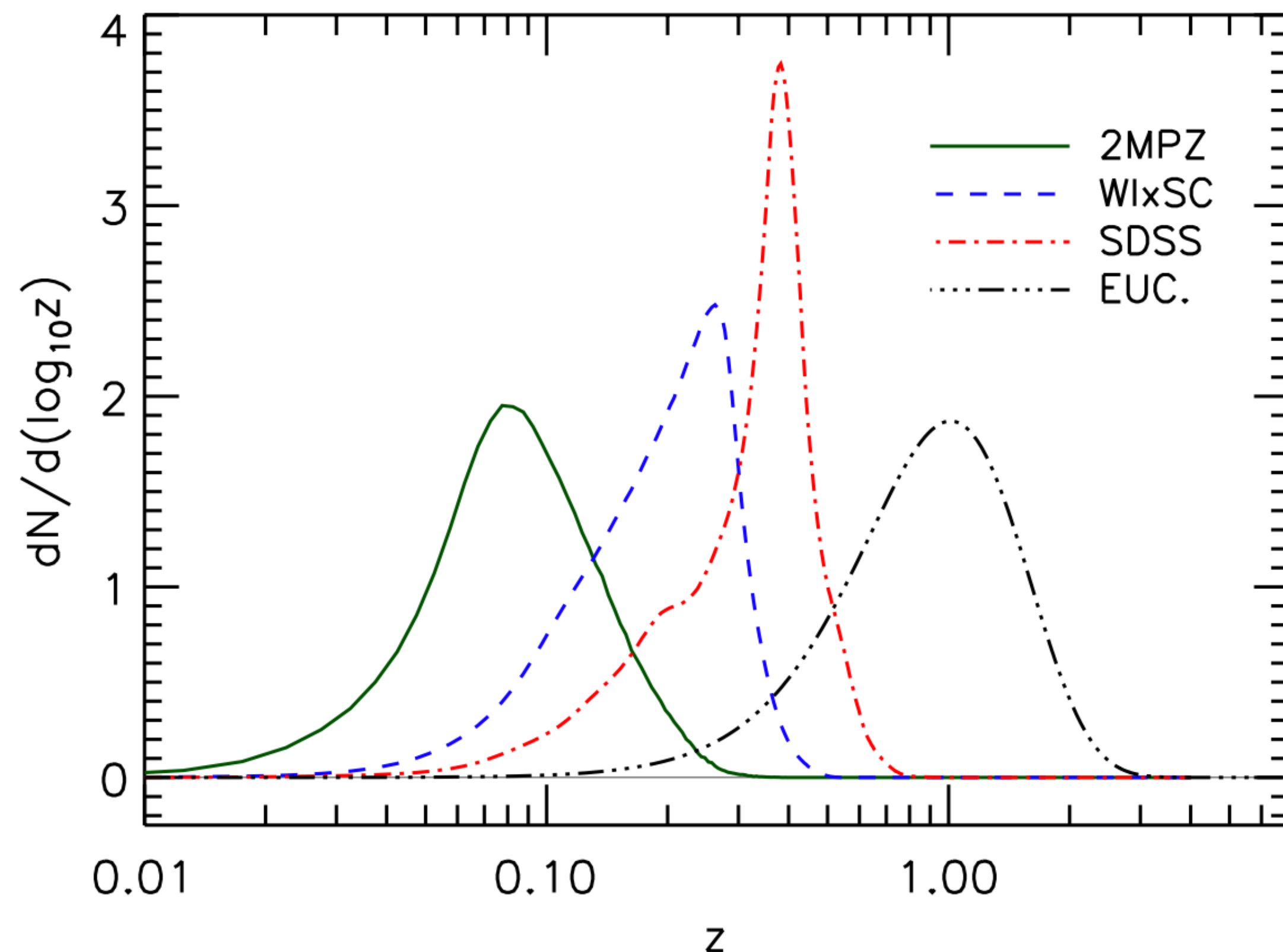


The galaxy catalogs

To reduce the *error on the x -correlation*, we want:

1. Large sky coverage
2. Large number of galaxies

Source redshift distribution



A. Cuoco et al., Astrophys. J. Suppl. 232, 1 (2017); L. Amendola et al., Living Rev. Rel. 21 (2018)

Future catalogs:

a. **EUCLID photometric catalog**

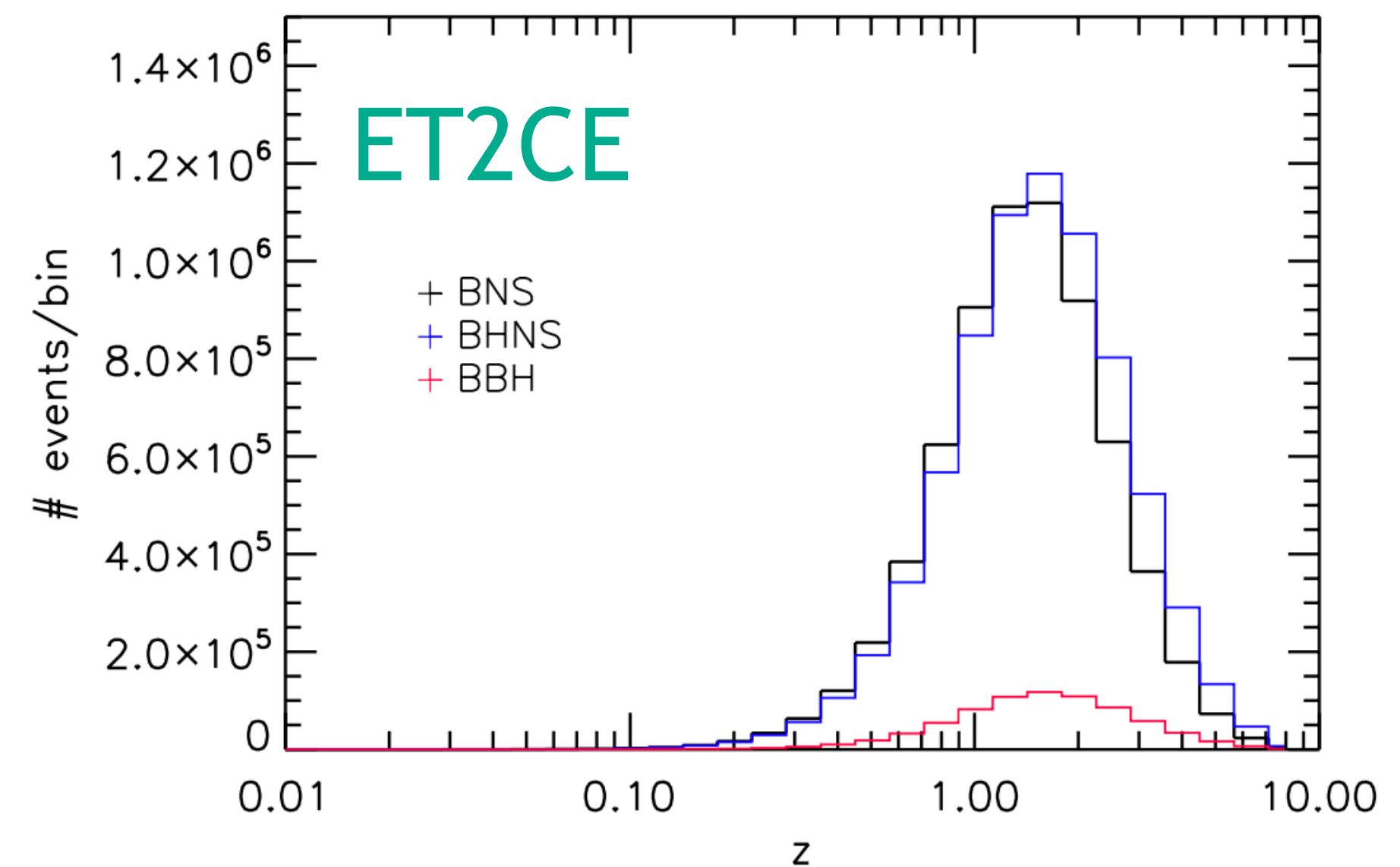
40% sky coverage, $\sim 1.6 \times 10^9$ galaxies

b. *Vera Rubin Obs (LSST)* photometric catalog

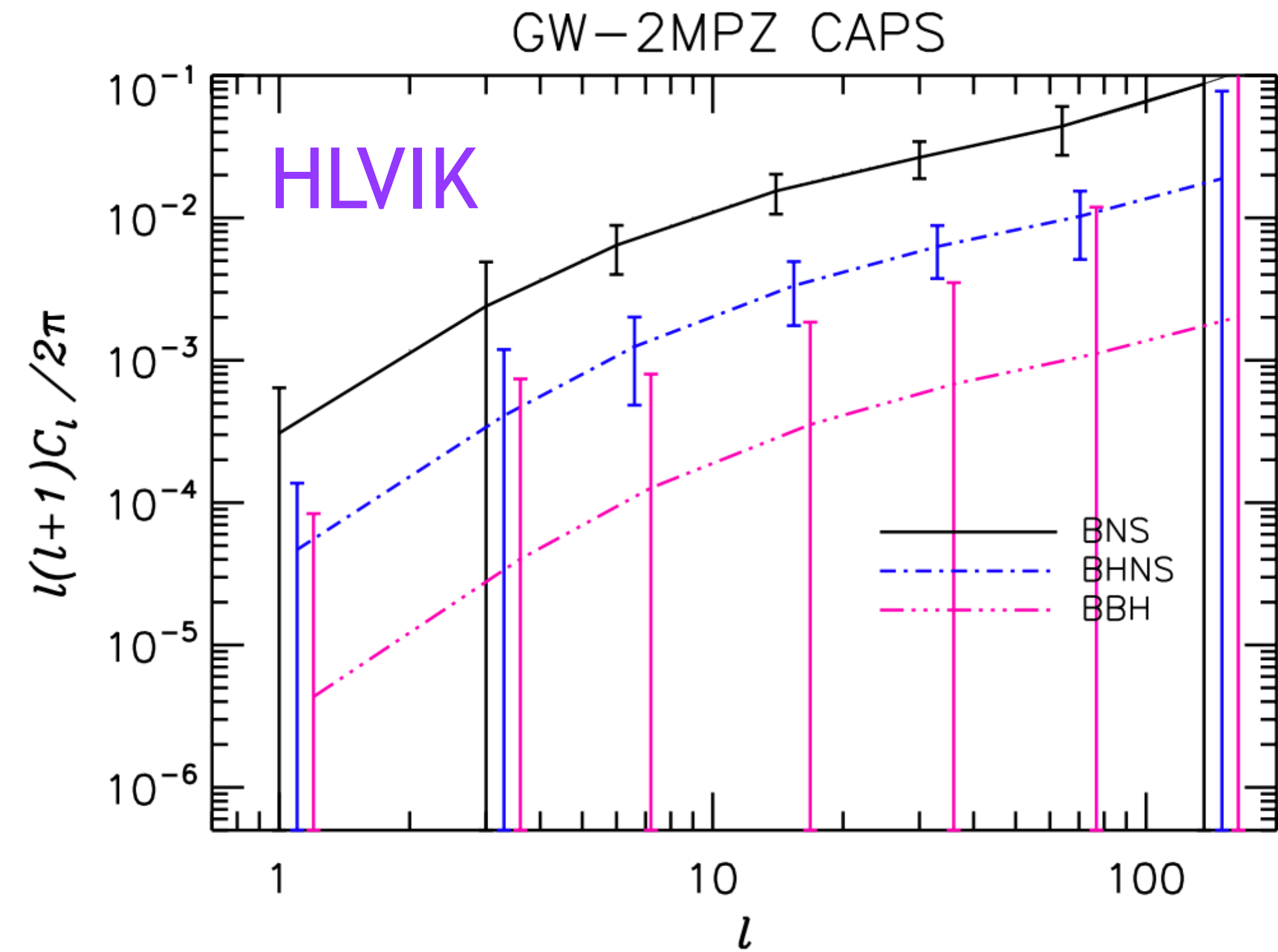
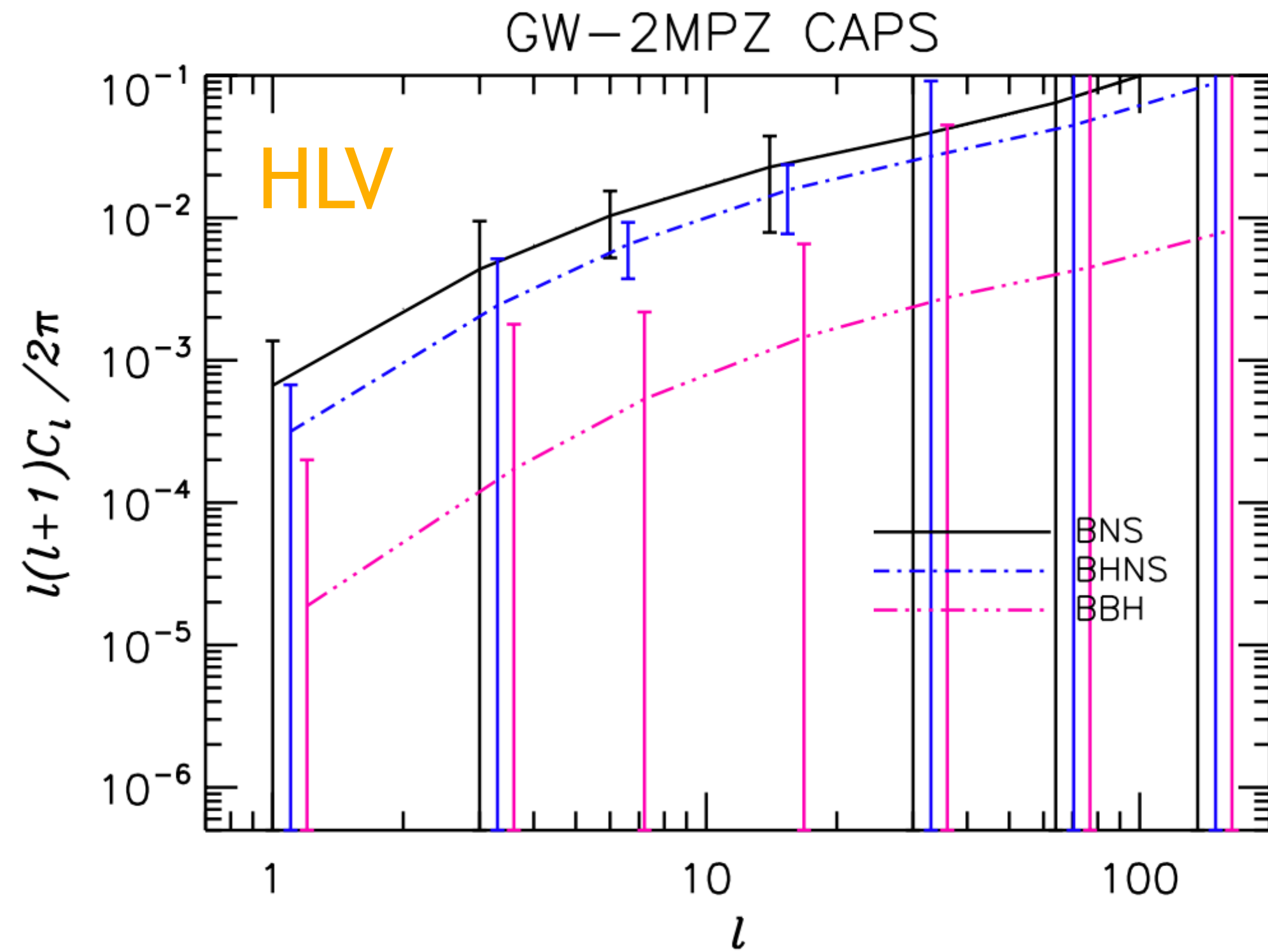
Similar to EUCLID performances

c. *SPHEREx*

Almost all-sky coverage, $\sim 10^9$ galaxies



Results I: cross-correlation of GW events



- **2MPZ** catalog provides the best performance because of the very good superposition of the redshift distributions, especially for **BNS** and **BHNS**
- However, x-correlation for **BBH** quite weak

Results I: cross-correlation of GW events

Significance of x-correlation

We quantify the significance of deviation from isotropy ($b = 0$), i.e. no x-correlation with LSS

Galaxy catalogs

Case	HLV			HLVIK		
Type	BNS	BBH	BHNS	BNS	BBH	BHNS
2MPZ	9	0.2	12	41	0.1	18
WlxSC	0.7	0.7	4	17	1.8	83
SDSS	0.0	0.4	1.0	2.4	1.4	19

Detectors
Binary populations

(Significance, σ)²

- **HLVIK** will detect x-correlation at more the 5σ for **BNS** (**BHNS**) with **2MPZ** (**WlxSC**)
- A 3σ signal for **BNS** (x**2MPZ**) is in the reach of **HLV**!
- For **BBH**, detection prospects are poorer because redshift distribution peaks at quite high z where anisotropy is small (volume effect) => *More events* are needed or....

Results II: cross-correlation of GW events

... A tomographic approach

EUCLID-like galaxy catalog x **BBH** events analysed in several redshift bins

Detectors

redshift bins

Case	HLV	HLVIK	ET2CE
0zbin	0.2	2.6	
2zbin	0.9	19	
3zbin	1.8	30	
5zbin	3.6	51	
9zbin			497
4zbin ($z > 1$)			101

(Significance, σ)²

- **HLV** will not show significant BBH x-correlation detection, about 2σ with 5 bins
- For **HLVIK**, *tomography is crucial*: detection possible at 4.3σ already with 2 bins!

Results II: cross-correlation of GW events

... A tomographic approach

EUCLID-like galaxy catalog x **BBH** events analysed in several redshift bins

Detectors

redshift bins

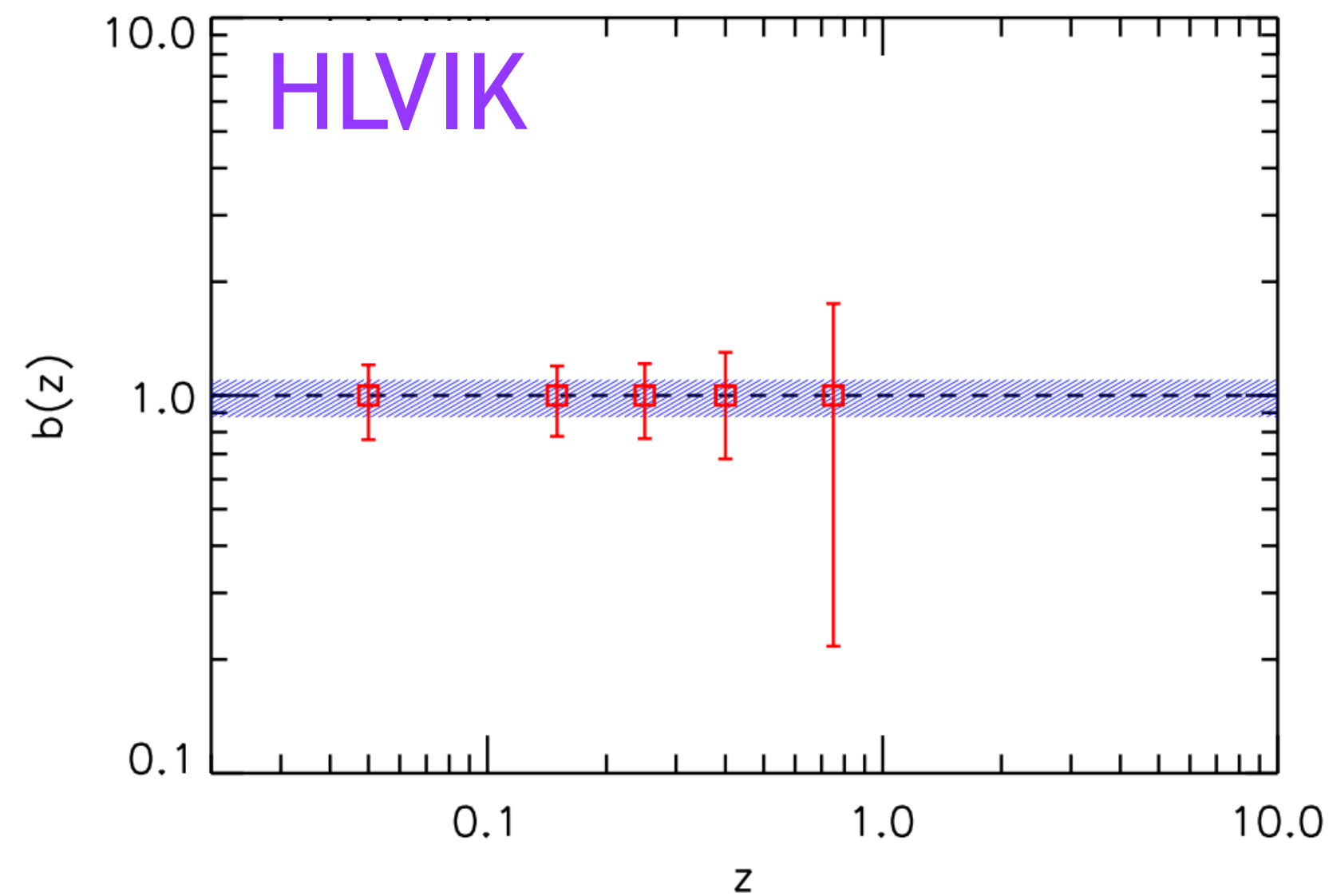
Case	HLV	HLVIK	ET2CE
0zbin	0.2	2.6	
2zbin	0.9	19	
3zbin	1.8	30	
5zbin	3.6	51	
9zbin			497
4zbin ($z > 1$)			101

(Significance, σ)²

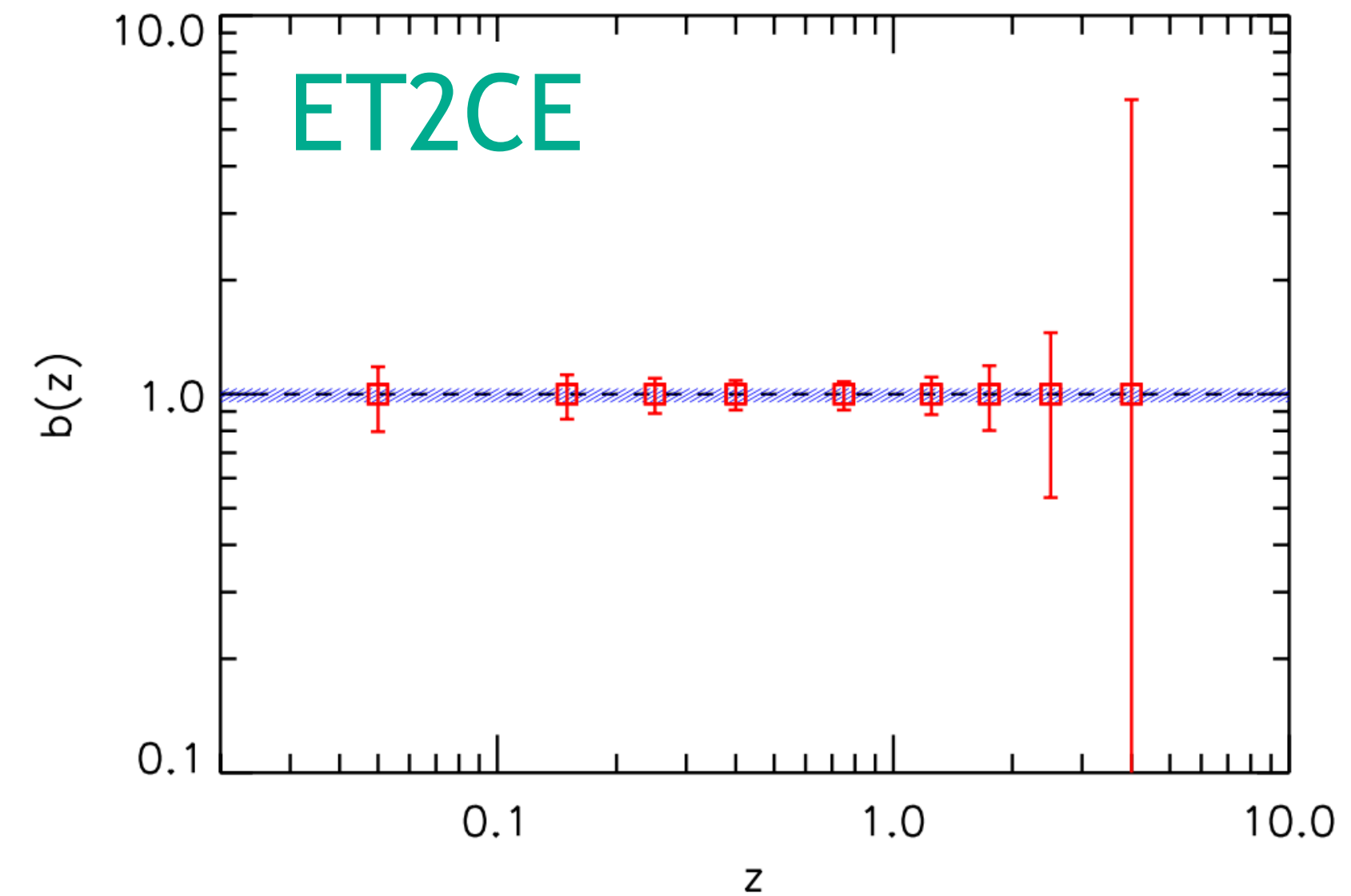
- **HLV** will not show significant BBH x-correlation detection, about 2σ with 5 bins
- For **HLVIK** is evident the the *crucial role of tomography*: detection possible at 4.3σ already with 2 bins only!
- **ET2CE** striking significance at 20σ for BBH-LSS correlation

Result III: BBH-LSS bias reconstruction

We quantify the (1σ) error on the reconstructed *bias*



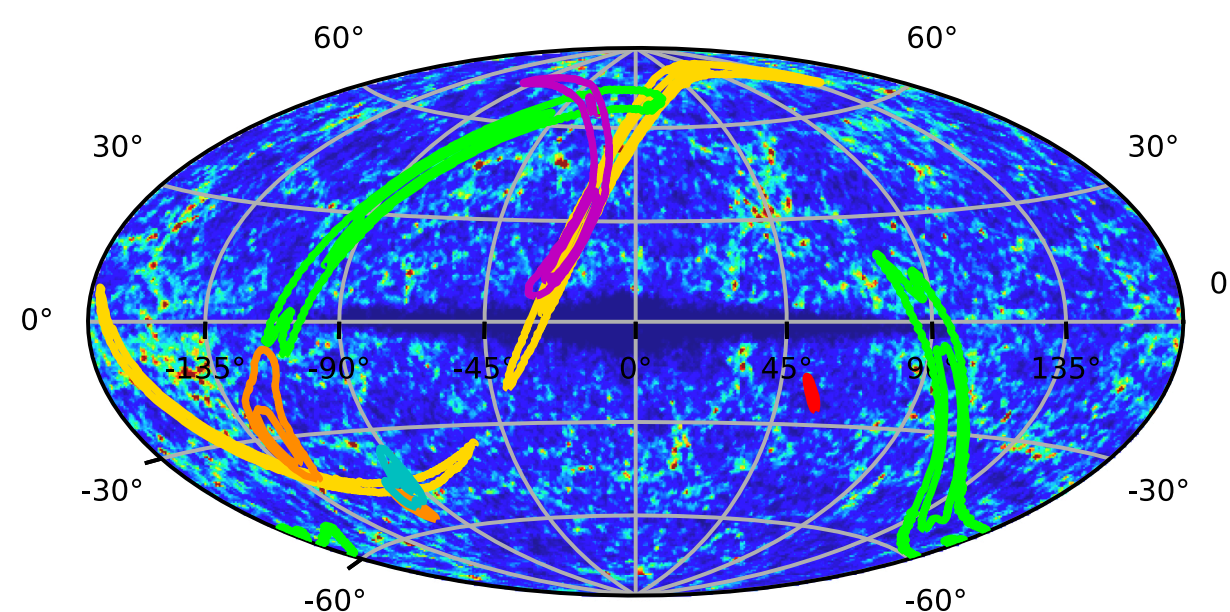
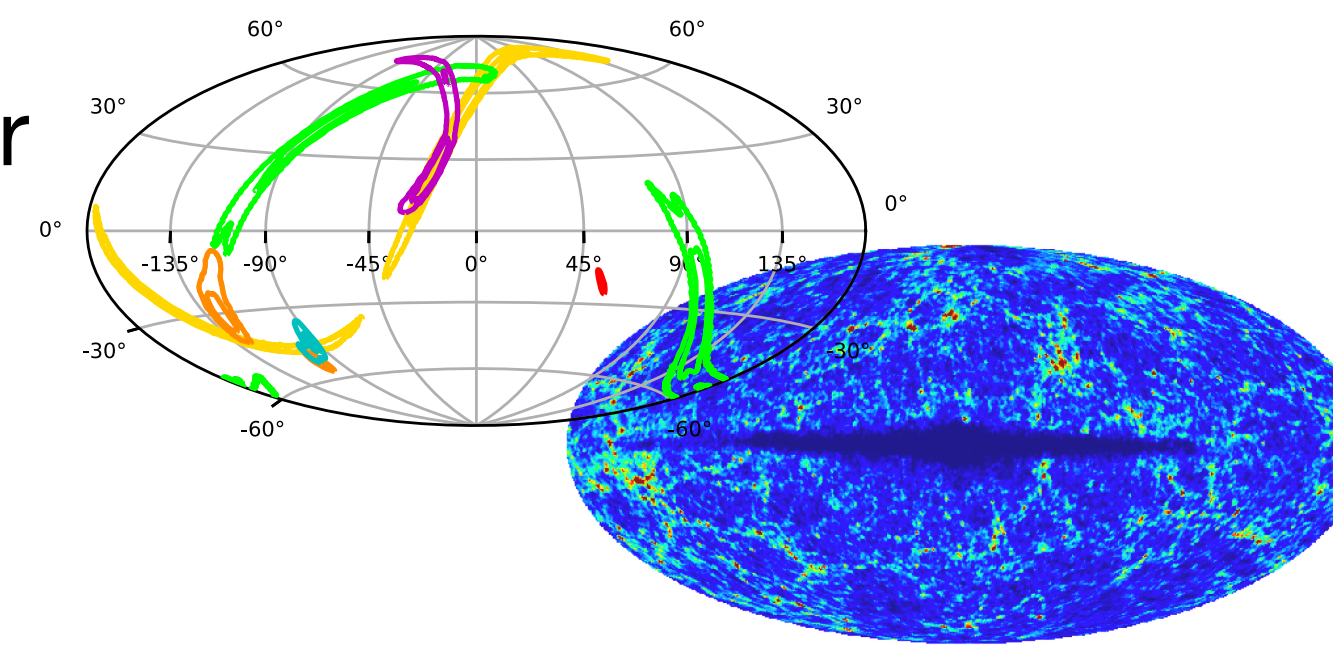
For **HLVIK**: single bin precision of about 20% at $z < 0.3$, down to 10% for combined analysis



For **ET2CE**: single bin error typically ~10% at low z , decreases to a few percent for $z \sim 0.5$; few % uncertainties for the combined analysis

Conclusions & Outlook

- Full simulation of the detectability **compact binary mergers populations** for specific detector configurations, fully accounting for instrumental effects (detection threshold, localisation error, etc)
- Use of current (and future) **galaxy catalogs** whose choice minimises the x-correlation error and guarantees maximum overlap in redshift distributions



- **HLVIK** will detect x-correlation at more the 5σ for **BNS** and **BHNS** with already available galaxy catalogs
- A 3σ signal for **BNS** is in the reach of **HLV!**
- For **BBH**, x-correlation significantly detected with current catalogs and **HLVIK** when a **tomographic approach** is adopted
- The BBH-LSS **bias** will be reconstructed with 10% (few %) accuracy with **HLVIK (ET2CE)**

- ➡ Discriminate different models at the origin of BBH (*stellar vs primordial*)
- ➡ Tomography also allows us to study *evolutionary effects* in the BBH population, if present
- ➡ Including *e.m. counterpart* informations will greatly enhance sensitivity for BNS and BHNS

Backup

Mock GW catalogs

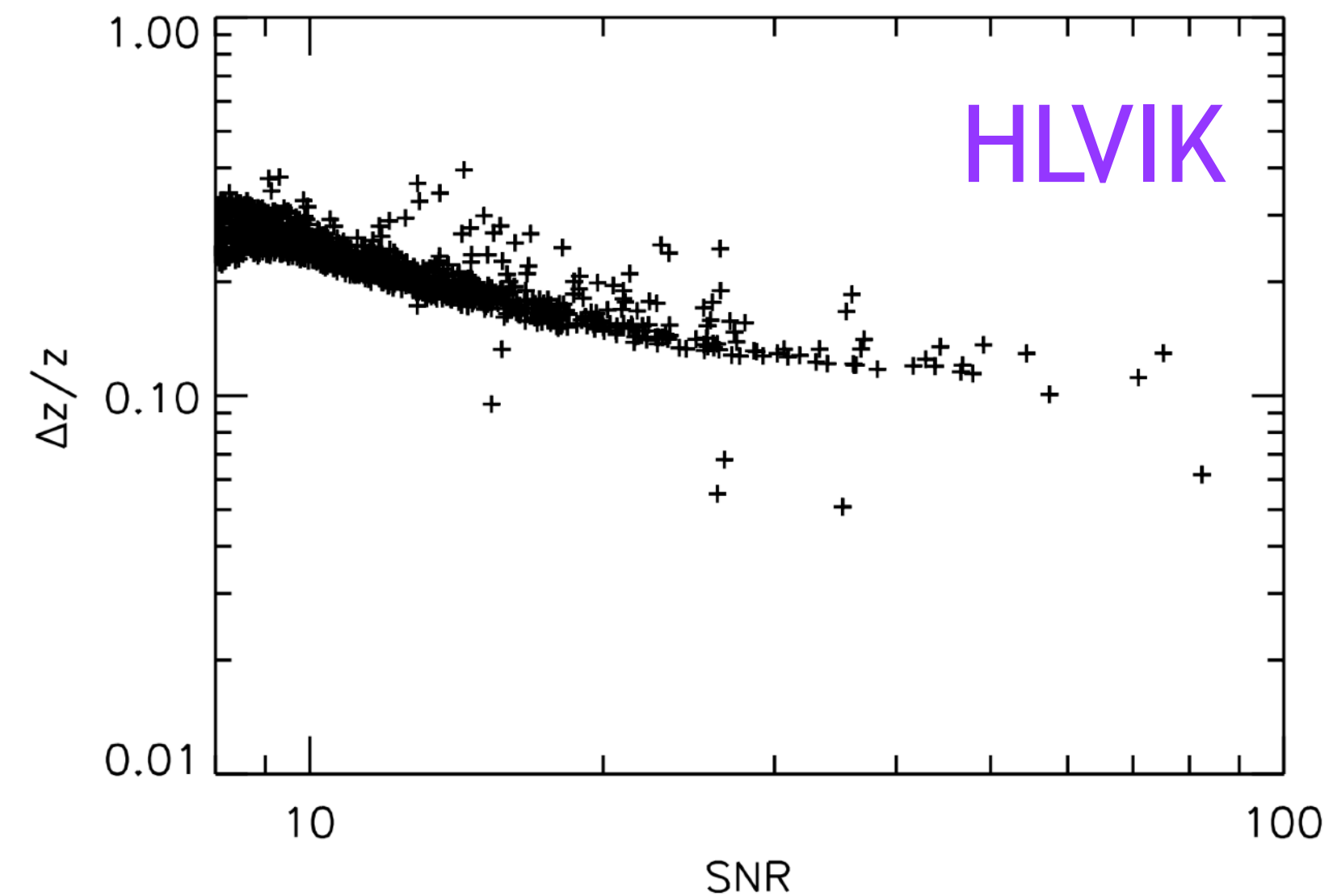
Positional reconstruction with *BAYESTAR*

Mock GW catalogs

Positional reconstruction with *BAYESTAR*

1. What is the error on the luminosity distance, i.e. redshift?

- 20-30% error on reconstructed redshift
- Relative error weakly dependent on SNR



Mock GW catalogs

Positional reconstruction with *BAYESTAR*

1. *What is the error on the luminosity distance, i.e. redshift?*

- 20-30% error on reconstructed redshift
- Relative error weakly dependent on SNR

2. *What is the beam shape?*

- Reasonably well localised events (i.e. better than $\sim 100 \text{ deg}^2$ at 50% C.L.) have posteriors well approximated by a 2D Gaussian
- Circular for **HLVIK**, but significantly elongated for **ET2CE**

Mock GW catalogs

Positional reconstruction with *BAYESTAR*

1. *What is the error on the luminosity distance, i.e. redshift?*

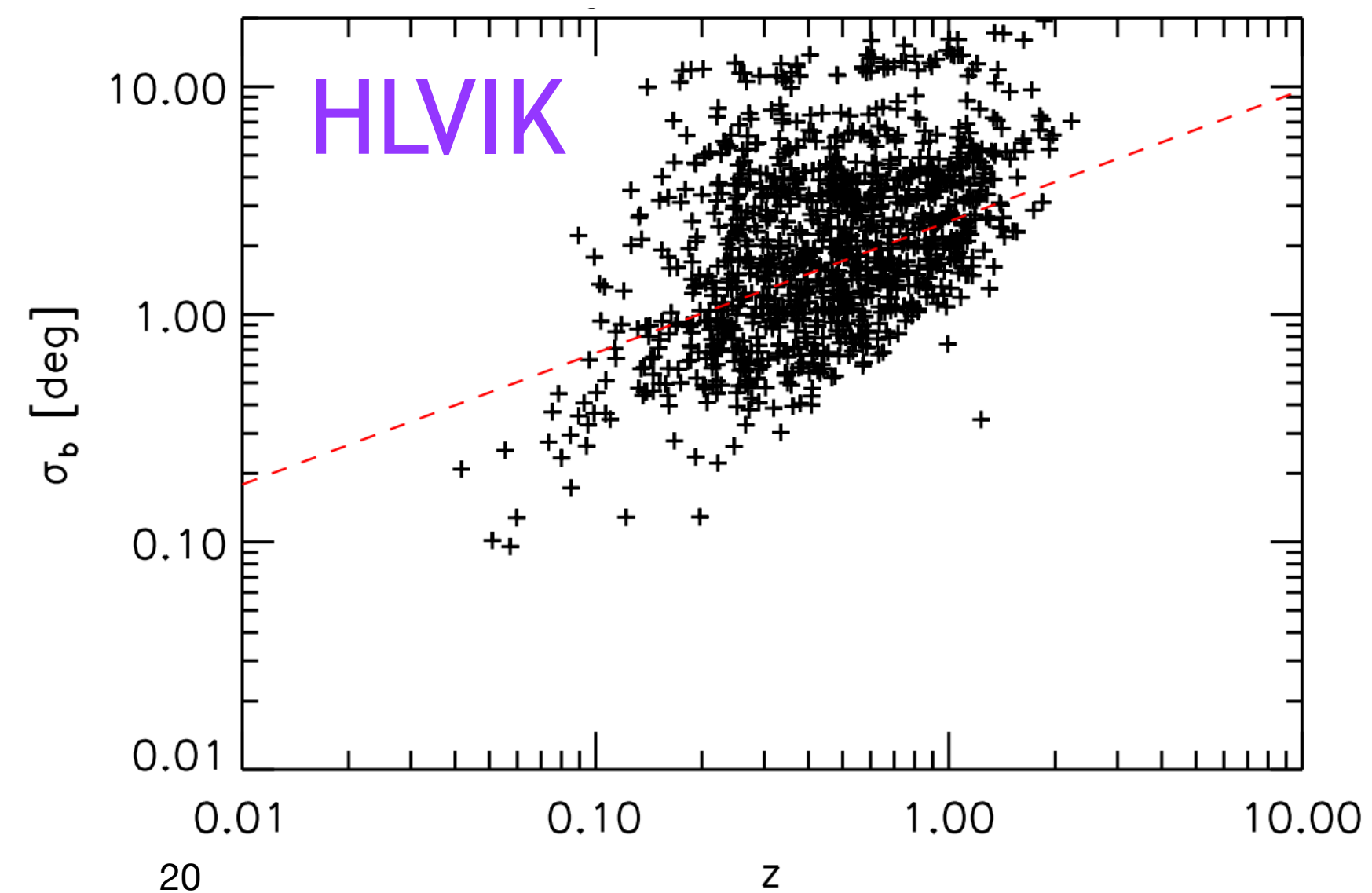
- 20-30% error on reconstructed redshift
- Relative error weakly dependent on SNR

2. *What is the beam shape?*

- Reasonably well localised events (i.e. better than $\sim 100 \text{ deg}^2$ at 50% C.L.) have posteriors well approximated by a 2D Gaussian
- Circular for **HLVIK**, but significantly elongated for **ET2CE**

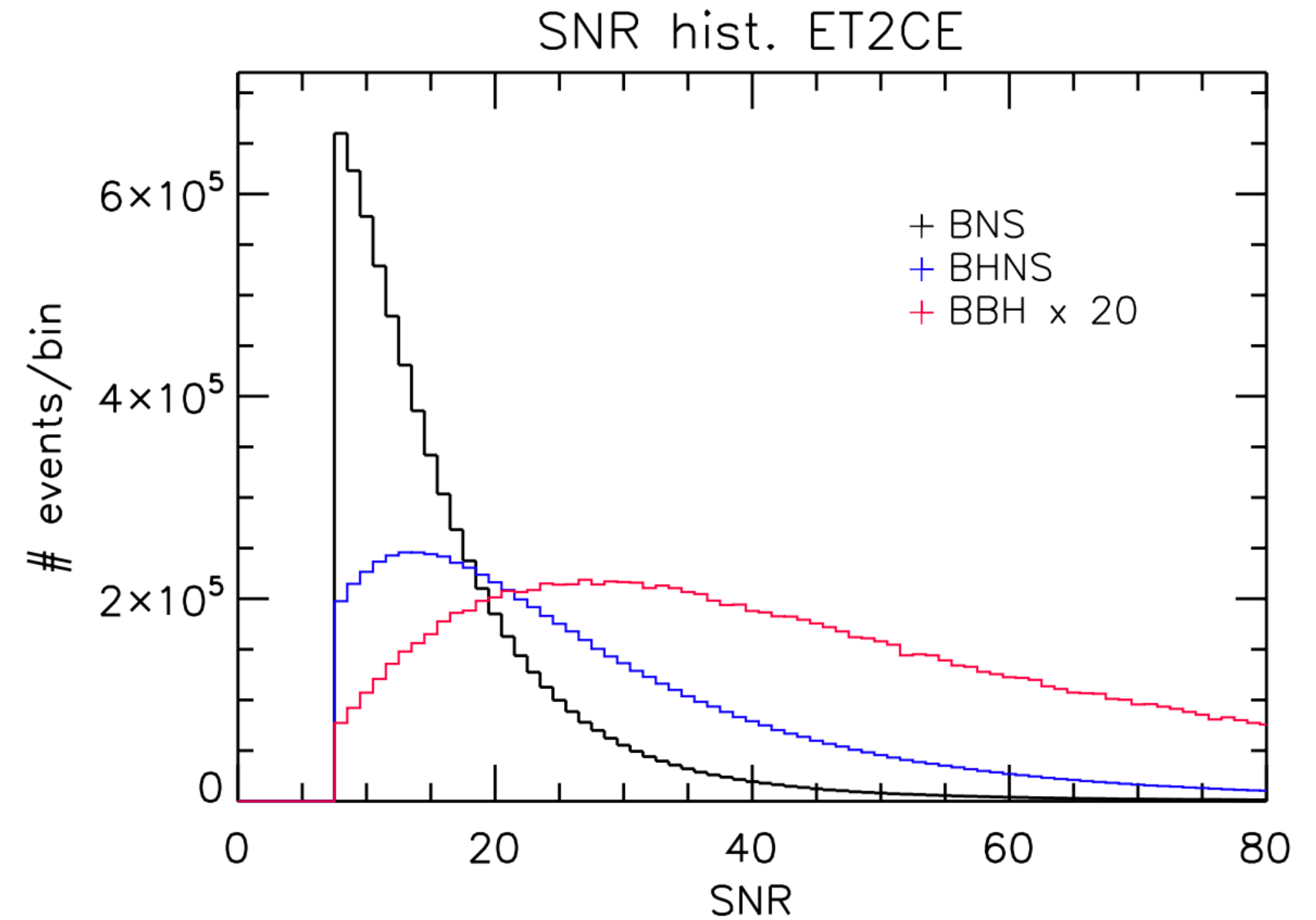
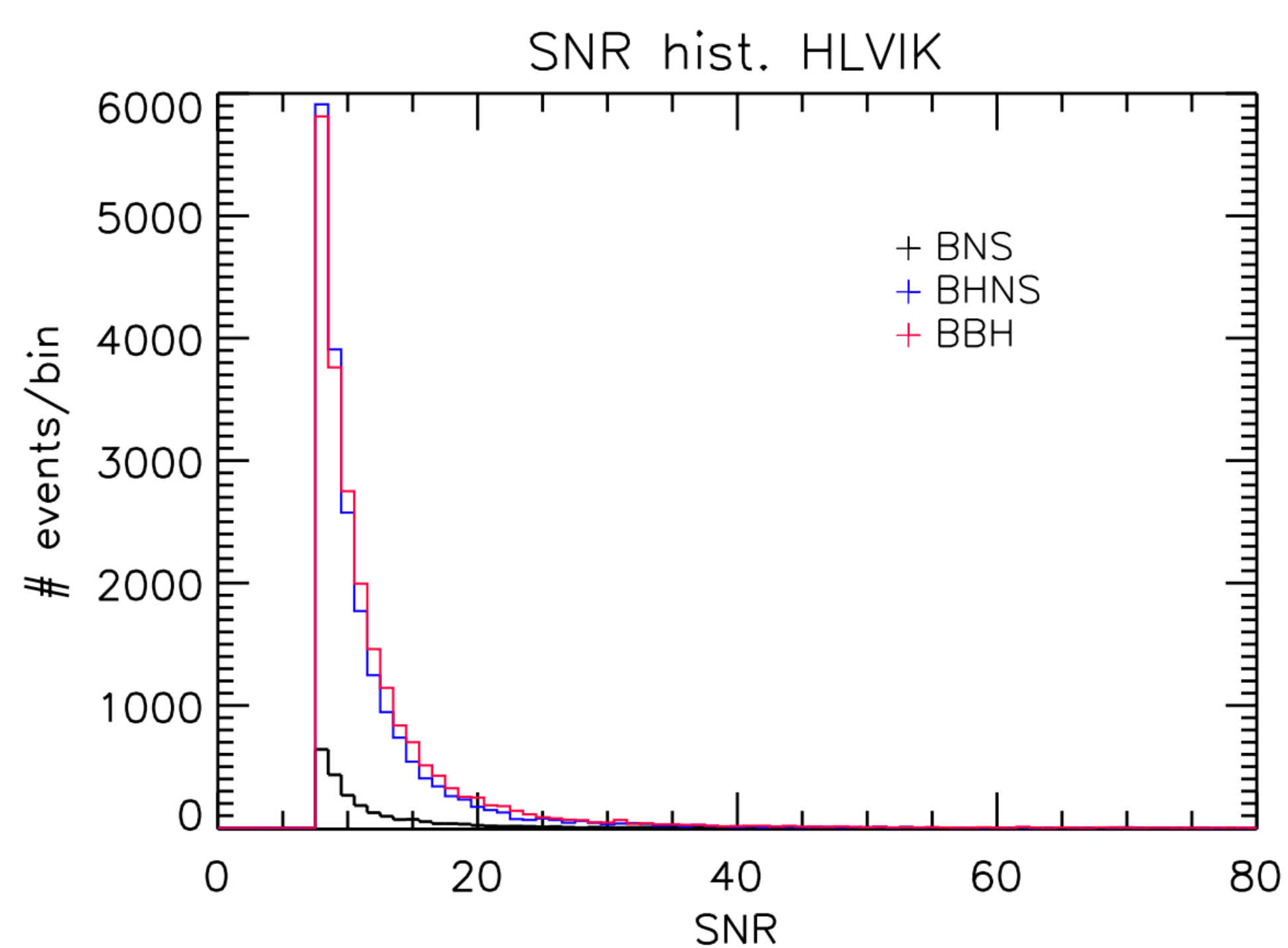
3. *What is the beam width?*

- Conversion of 50% C.L. localisation area in circular Gaussian beam for **HLVIK** and **ET2CE**
- Quality cuts and redshift dependence
- For **HLV**, 4 deg width w/ no redshift dependence



ET2CE: BBH vs BNS event quality reconstruction

BNS larger fraction of events with poor angular resolution makes ET2CE performance more similar to HLVIK ones



SNR distribution of BNS ET2CE is peaked at low SNR, qualitatively similar to the event distribution of the HLVIK

BBH is peaked at SNR ~ 30 , i.e. the BBH sample seen by ET2EC is virtually complete, with the improved sensitivity resulting in stronger signals

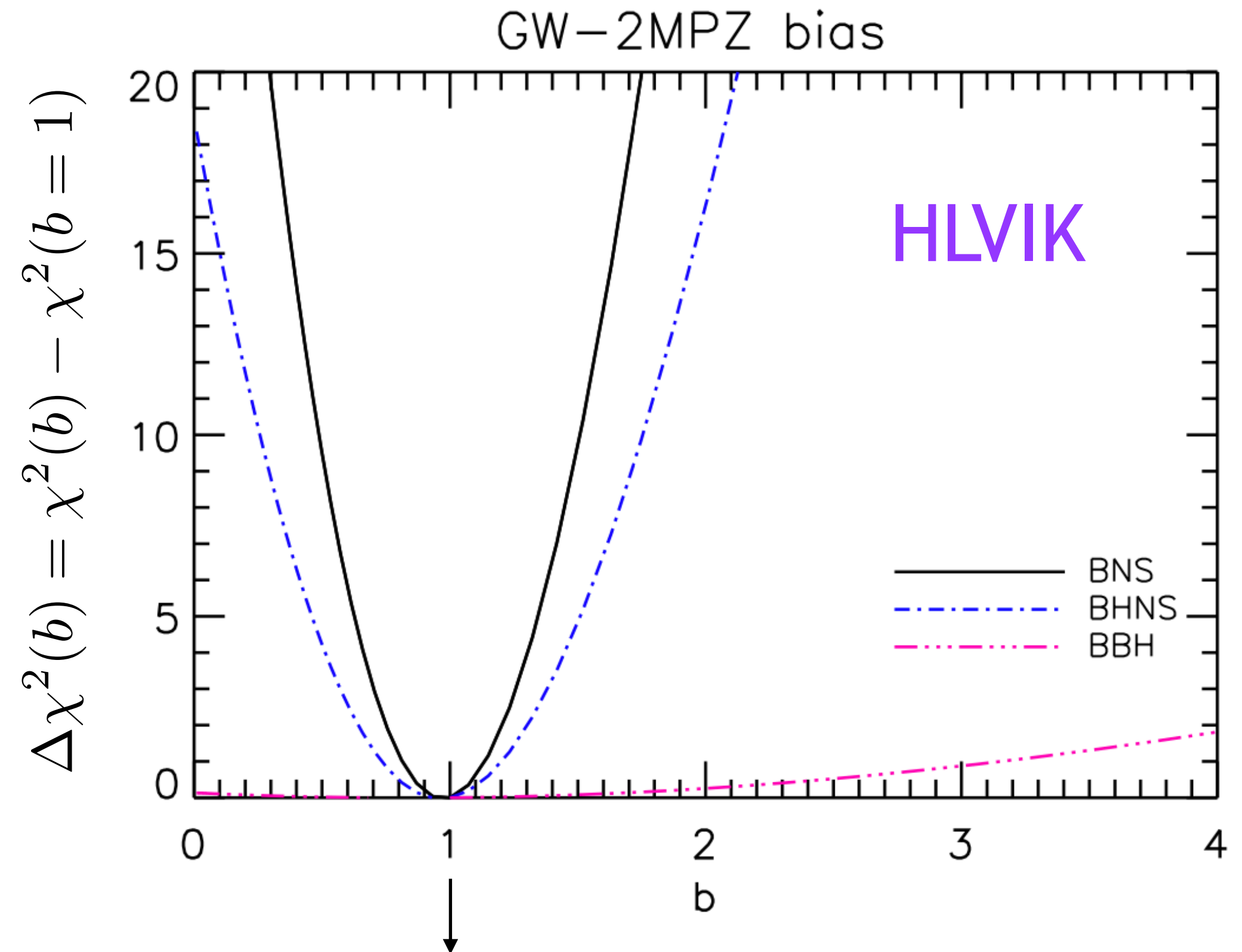
=> Apart for improved statistics, **we do not expect the ET2EC sample of BNS to show qualitatively new features with respect to HLVIK**

Cross-correlation of GW events

Statistical framework

$$\chi^2(b) = \sum_{j,\ell} \left[\frac{C_{\ell,j}^{ab}(b=1) - C_{\ell,j}^{ab}(b)}{\delta C_{\ell,j}^{ab}(b)} \right]^2$$

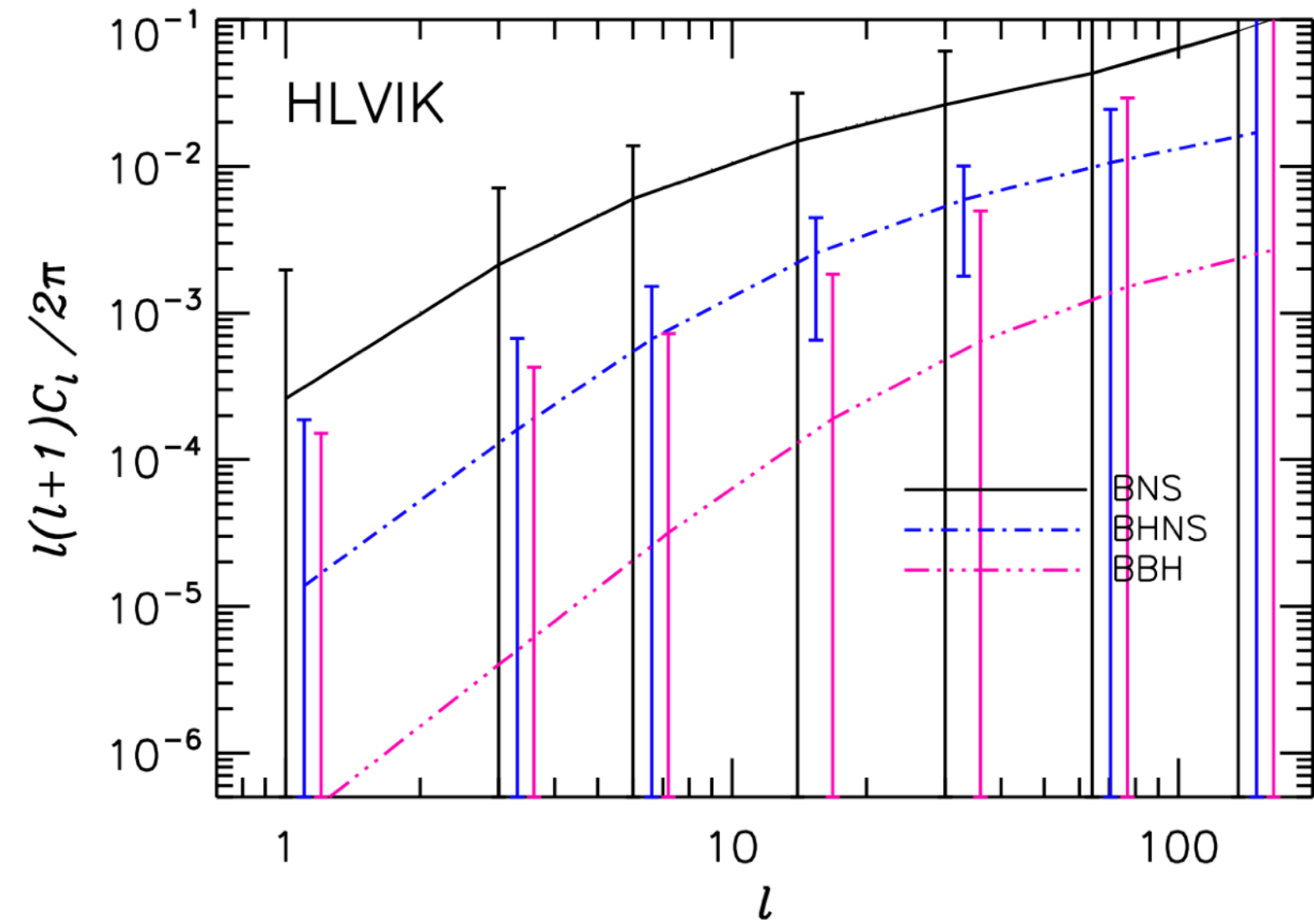
1. $\Delta\chi^2(b)$: used to compute the one sigma error on b , when $\Delta\chi^2=1$ around $b = 1$
2. $\Delta\chi^2(b=0)$: used to quantify the statistical significance, in σ 's, of the cross-correlation with respect to the isotropic sky ($b = 0$)**



Our reference model assumes that GW events are an unbiased tracer ($b = 1$) of LSS

** $b=0$ is a nested case with respect to the model with b as free parameter

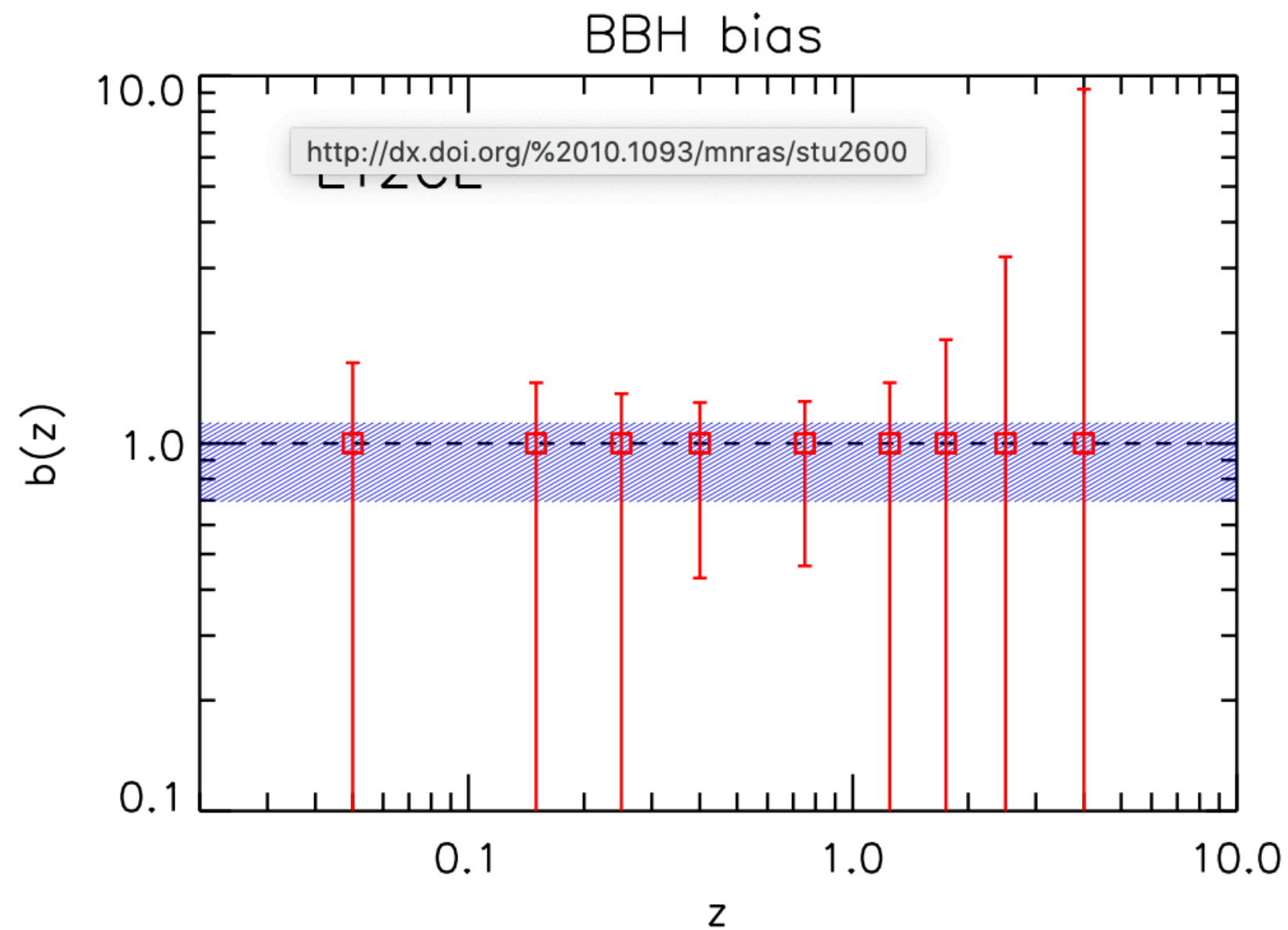
Results: auto-correlation of GW events



Normalisation of the APS is larger in the BNS case

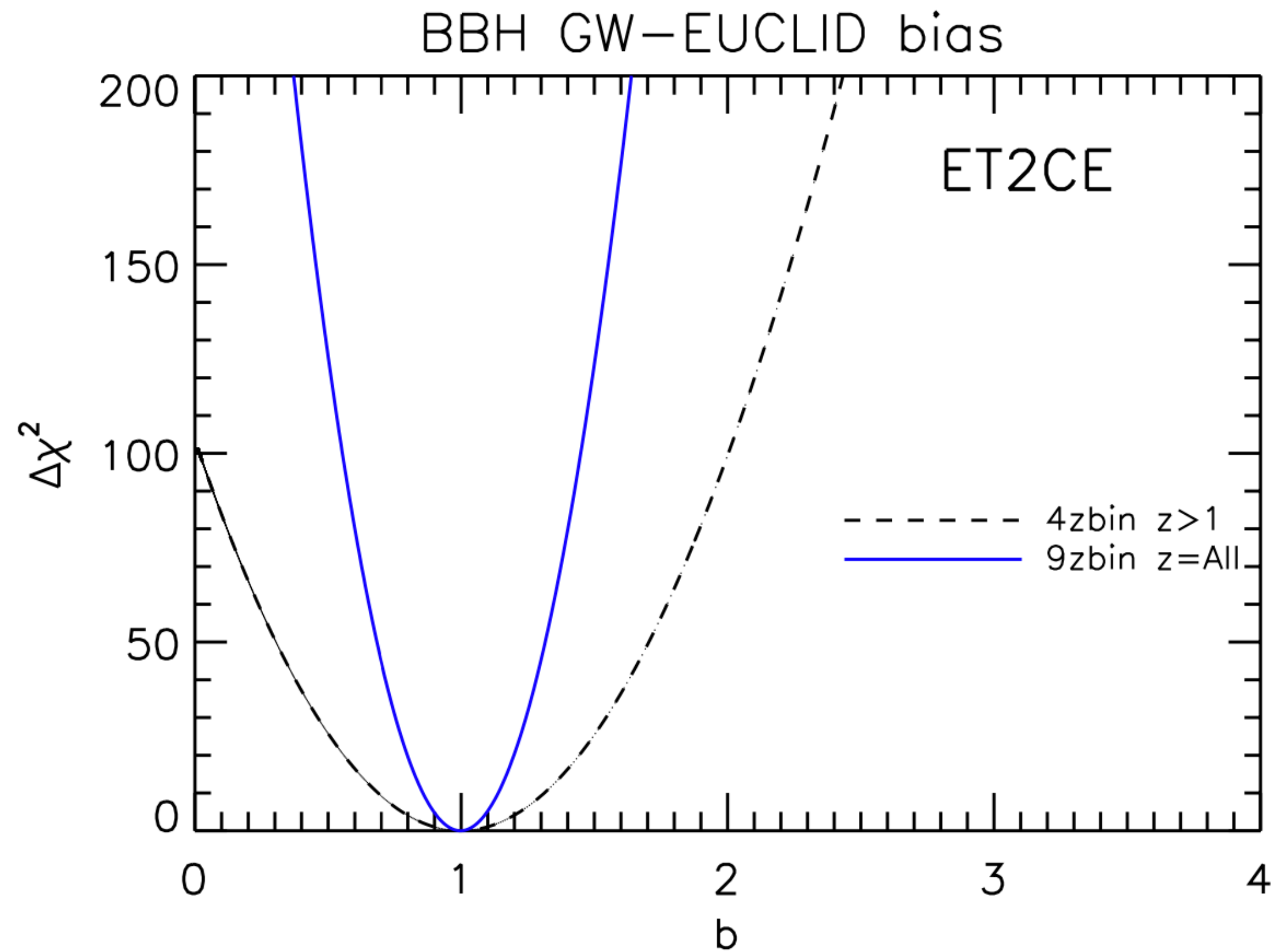
Purely volume effect. In the cases of BBH and BHNS, which extend to larger redshifts, the averaging over a larger volume reduces the final anisotropy and thus the APS normalisation

However, the total number of events is also important in assessing the error with which a measurement can be performed



Large errors on bias reconstruction

Results: the relevance of low-z events



Not considering low-z events dramatically decreases the significance of the detection (from about 20σ to 10σ), even if only $\sim 20\%$ of the events are at $z < 1$

G. Scelfo et al., JCAP 1809, 039 (2018), arXiv:1809.03528